Aus dem Institut für Muskuloskelettale Medizin (MUM)
Klinik der Universität München

Direktor: Prof. Dr. med. Boris Holzapfel

Fundamentals for the journey towards an enhanced understanding of human patello-femoral joint mechanics

Dissertation

zum Erwerb des Doktorgrades der Humanbiologie

an der Medizinischen Fakultät der

Ludwig-Maximilians-Universität zu München

vorgelegt von

Adrian Sauer

aus

Oberkirch

2023

Berichterstatter:	Prof. Dr. med. habil. Dr.-Ing. Thomas M. Grupp, FIOR
Mitberichterstatter:	Prof. Dr. Hans Hertlein
	Prof. Dr. Steffen Peldschus
Mitbetreuung durch den promovierten Mitarbeiter:	PD Dr. Dipl.-Ing. (FH) Matthias Woiczinski
Dekan:	Prof. Dr. med. Thomas Gudermann
Tag der mündlichen Prüfung:	04.10.2023

Affidavit

Eidesstattliche Versicherung

Sauer, Adrian
_____
Name, Vorname

Ich erkläre hiermit an Eides statt, dass ich die vorliegende Dissertation mit dem Titel:

Fundamentals for the journey towards an enhanced understanding of human patello-femoral joint mechanics

selbständig verfasst, mich außer der angegebenen keiner weiteren Hilfsmittel bedient und alle Erkenntnisse, die aus dem Schrifttum ganz oder annähernd übernommen sind, als solche kenntlich gemacht und nach ihrer Herkunft unter Bezeichnung der Fundstelle ein-zeln nachgewiesen habe.

Ich erkläre des Weiteren, dass die hier vorgelegte Dissertation nicht in gleicher oder in ähnli-cher Form bei einer anderen Stelle zur Erlangung eines akademischen Grades eingereicht wurde.

Oberkirch, 05.10.2023   Adrian Sauer
_____   _____
Ort, Datum   Unterschrift Doktorandin bzw. Doktorand

Acknowledgements

While working on this dissertation, a lot more time passed by than I expected initially. This long period of time – nearly six years – were years in which I learned and struggled a lot and at every point in time, in every situation there were people around me who gave me great support!

First, I want to thank BBraun and my supervisors Thomas Grupp and Allan Maas, who gave me the possibility to start this project, to find my own way to work on it and to develop my own abilities on this journey.

Additionally, I want to thank all my colleagues and friends who supported me a lot. Especially I want to thank…

Ronja, who was the perfect example to follow in the past few years and who listened to me, when I questioned the whole project,

Ariana, who finally brought fun and some passion into my scientific work,

Matthias, who encouraged me to believe in the value of our work and

Andi and Tobi who introduced me into the world of programming.

Most importantly, I want to thank my whole family for the last 32 years which made me what I am today:

My dad taught me to do things right.

My mum taught me to do things with love.

My brother taught me to do things together.

Larissa taught me to sometimes don't do things and

Nino taught me a lot about priorities in life.

Table of contents

List of abbreviations

AKP .... Anterior knee pain

BW...Body weight

TKA .... Total knee arthroplasty

UHMWPE .... Ultra-high-molecular-weight polyethylene

List of publications

I.   Publications as part of the cumulative dissertation

Sauer A, Maas A, Ottawa S, Giurea A, Grupp T M. Towards a New, Pre-Clinical, Subject-Independent Test Model for Kinematic Analysis after Total Knee Arthroplasty—Influence of the Proximo-Distal Patella Position and Patellar Tendon Stiffness, Journal of applied sciences 2021, 11(21), 10322. DOI: 10.3390/app112110322

Sauer A, Kebbach M, Maas A, Mihalko W M, Grupp T M. The Influence of Mathematical Definitions on Patellar Kinematics Representations, Materials 2021, 14(24), 7644. DOI: 10.3390/ma14247644

Sauer A, Thorwaechter C, Dupraz I, Maas A, Steinbrueck A, Grupp T M, Woiczinski M. Isolated effects of patellar resurfacing in total knee arthroplasty and their relation to native patellar geometry, Nature Scientific Research 2022, 12 (1), 12979. DOI: 10.1038/s41598-022-16810-2

II.   Additional publications

Sporer E M, Schilling C, Sauer A, Tait R T, Giurea A, Grupp T M. Biomechanical Effects of stemmed total knee arthroplasty on the human femur: a CT-data based study, BioMed Research International 2022, 5738610. DOI: 10.1155/2022/5738610

Ortigas Vásquez A, Taylor W R, Maas A, Woiczinski M, Grupp T M, Sauer A. A Frame Orientation Optimisation Approach for Consistent Interpretation of Kinematic Signals. Submitted 2023.

III.   Podium presentations

Sauer A, Maas A, Grupp T M (2019). FE-Kniemodell auf Grundlage standardisierter Lastdaten, *IX. Münchener Symposium für Experimentelle Orthopädie, Unfallchirurgie und Muskuloskelettale Forschung, February 28 - March 1, Munich, Germany*

Sporer E M, Schilling C, Sauer A, Tait R T, Giurea A, Grupp T M (2021). Targeting End-of-Stem Pain: A Biomechanical Analysis Based on 3-Dimensional Models of Human Femora. *26th Congress of the European Society of Biomechanics, July 12 - 14, Milan, Italy.*

Sauer A, Ortigas-Vásquez A, Maas A, Grupp T M (2022). Einfluss der Achsenausrichtung auf Kinematikdaten – Auswirkungen und ein Ansatz zur Standardisierung. *12. Kongress der Deutschen Gesellschaft für Biomechanik (DGfB), September 28 - 30, Cologne, Germany.*

Sauer A, Thorwächter C, Dupraz I, Maas A, Steinbrück A, Grupp T, **Woiczinski M** (2022). Rundes Patelladesign vs. Ovales Patelladesign beim Patellarückflächenersatz. *12. Kongress der Deutschen Gesellschaft für Biomechanik (DGfB), September 28 - 30, Cologne, Germany.*

IV. Poster presentations

Sauer A, Maas A, Grupp T M (2018). A method for FE-analysis of knee kinematics based on standardized loads. *8th World Congress of Biomechanics, July 8 - 12, Dublin, Ireland.*

Sauer A, Maas A, Grupp T M (2018). A method for FE-analysis of knee kinematics based on standardized loads. *11. Kongress der Deutschen Gesellschaft für Biomechanik (DGfB), April 3 - 5, Berlin, Germany.*

Ortigas Vásquez A, Sauer A, Maas A, Taylor W R, Grupp T M (2023). Standardising frame alignments to allow for consistent kinematic interpretation: part I. *18th International Symposium on Computer Methods in Biomechanics and Biomedical Engineering, May 3 - 5, Paris, France.*

Sauer A, Ortigas Vásquez A, Maas A, Taylor W R, Grupp T M (2023). Standardising frame alignments to allow for consistent kinematic interpretation: part II. *18th International Symposium on Computer Methods in Biomechanics and Biomedical Engineering, May 3 - 5, Paris, France.*

Author contributions

The contributions of all co-authors to the three publications of this cumulative dissertation are confirmed and submitted separately. All authors agreed that these publications are used within this dissertation and must not be part of another doctoral thesis.

I.   Contributions to publication I

For the first publication (*"Towards a New, Pre-Clinical, Subject-Independent Test Model for Kinematic Analysis after Total Knee Arthroplasty—Influence of the Proximo-Distal Patella Position and Patellar Tendon Stiffness"*, Journal of applied sciences, 2021) the author of this dissertation contributed substantially to the concept and methodology, to the validation and the formal analyses, as well as the draft of the manuscript and the figures.

II.   Contributions to publication II

For the second publication (*"The Influence of Mathematical Definitions on Patellar Kinematics Representations"*, materials, 2021) the author of this dissertation contributed substantially to the concept and methodology, to the validation and the formal analyses, as well as the draft of the manuscript and the figures. The software to transform between kinematic conventions provided as supplementary material to this publication was written by the author of this dissertation.

III.   Contributions to publication III

For the third publication (*"Isolated effects of patellar resurfacing in total knee arthroplasty and their relation to native patellar geometry"*, Nature scientific reports, 2022) the author of this dissertation contributed substantially to the conceptualisation and the execution of the tests. The methodology of the tests on the knee-rig was previously established. The author also contributed to the raw data processing and the formal analyses as well as the draft of the manuscript and the figures.

1. Abstract (German):

Hintergrund

Anteriorer Knieschmerz ist eine der Hauptursachen für Unzufriedenheit bei Patienten mit einer Knie-Totalendoprothese. Da anteriorer Knieschmerz im Patellofemoralgelenk und seiner direkten Umgebung lokalisiert ist, ist es sehr wahrscheinlich, dass seine Ursache in diesem Gelenk zu suchen ist. Die Kombination von Studien zu patellofemoralen Kontaktkräften und zu Verschleißtests von künstlichen Patellakomponenten kann zu Schlussfolgerungen führen, die nicht mit den vergleichsweise niedrigen Revisionsraten von Patellaimplantaten aus aktuellen Registerdaten in Einklang zu bringen sind. Dieser Widerspruch zeigt den Bedarf nach einem besseren Verständnis der Mechanik des Kniegelenks, insbesondere des Patellofemoralgelenks. Dies könnte in Zukunft ein Schlüsselfaktor sein, um die Auftretenshäufigkeit von anterioren Knieschmerzen zu reduzieren.

Zielsetzung

Primäres Ziel dieser Dissertation ist es, das Verständnis der patellofemoralen Gelenkmechanik durch Anwendung eines neuen Ansatzes zur Simulation des Kniegelenks zu verbessern. Dieser neue Ansatz zielt darauf ab, die Abhängigkeit der Simulationsergebnisse von häufig nur näherungsweise bestimmbaren Parametern zu reduzieren. Zur Validierung dieses Modells muss die patellofemorale Kinematik näher analysiert und besser verstanden werden. Daraus ergibt sich das zweite Ziel dieser Arbeit, das im Schaffen der Grundlagen für den mathematisch sorgfältigen Umgang mit patellofemoralen Kinematikdaten liegt. Darauf aufbauend wird die Untersuchung von Einflussfaktoren auf die Patellakinematik vorangetrieben. Dabei wird zunächst der Effekt der Verwendung eines Patellarückflächenersatzes auf die Patellakinematik in einer humanen Präparatstudie isoliert.

Material und Methoden

In einem ersten Schritt wurde ein Finite-Elemente-Modell entwickelt, das auf standardisierten in-vivo Lastdaten des Tibiofemoralgelenks beruht. Da diese Daten implizit alle Kräfte und Momente, die durch Gravitation, Dynamik und den tibio-femoralen Gelenkspalt überquerende Bänder und Sehnen induziert werden enthalten, kann in diesem neuartigen Modell auf die explizite Modellierung der Mehrheit dieser Elemente verzichtet werden, ohne die Validität des Modells zu reduzieren. Dieses Modell wurde zur Analyse der Effekte der initialen proximo-distalen Patellaposition und der Steifigkeit des Patellabandes auf die Kinematik der Patella eingesetzt.

Im zweiten Teil dieser Dissertation wurde ein grundlegenderes Thema bearbeitet, indem Methoden zur präzisen Analyse und Interpretation von Patellakinematikdaten neu etabliert

wurden. Die Darstellung von Kinematikdaten, insbesondere der patellofemoralen Rotationen, ist stark von den zugrundliegenden mathematischen Methoden und deren exakter Anwendung abhängig. Eine Zusammenstellung der am häufigsten verwendeten Konventionen zur Beschreibung patellofemoraler Rotationen wurde erstellt und Methoden zur exakten Konvertierung von Daten zwischen diesen Konventionen entwickelt. Diese wurden der Allgemeinheit in Form einer Software zur Verfügung gestellt.

Um die Auswirkungen der Parameter, die die Patellakinematik beeinflussen, besser zu verstehen, wurden die Effekte des Einsatzes von Patellarückflächenimplantaten aus In-vitro-Tests mit acht Humanpräparaten auf einem etablierten Kniegelenkskinemator am Muskuloskelettalen Universitätszentrum München (MUM) isoliert. Um die spezifischen Auswirkungen des Patellaimplantats zu identifizieren, wurde die Kniekinematik vor und nach der TKA mit und ohne Patellarückflächenersatz für zwei tibio-femorale Implantatvarianten (posterior stabilisiertes PS und PS+) gemessen und verglichen.

Ergebnisse

Das Finite-Elemente-Modell ermöglicht vergleichende Studien mit verschiedenen Implantaten oder Parametern. Für das Tibiofemoralgelenk stimmen sowohl die Kinematik als auch die Kontaktsituation mit Ergebnissen aus der bestehenden Literatur überein. Für das Patellofemoralgelenk wurde gezeigt, dass die initial mehr proximale Position der Patella und eine schwächere Patellasehne zu erhöhter Patellaflexion und -rotation führen, während der Shift und Tilt der Patella stärker von der initialen Patellaposition beeinflusst sind.

Die Analyse der zugrundeliegenden mathematischen Konventionen für die Darstellung patellofemoraler Rotationen zeigt, dass sowohl die Absolutwerte als auch die Charakteristik der Kurven grundlegend durch die Wahl der Konvention beeinflusst werden. Die entwickelten Methoden zur Transformation von Daten zwischen den betrachteten Konventionen wurden mittels mathematischer Beweise und eines Vergleichs mit Referenzdaten validiert.

Im experimentellen Teil dieser Dissertation konnten keine signifikanten Effekte durch den Einsatz eines Patellarückflächenersatzes auf die Rotationen der Patella festgestellt werden. Bei Betrachtung der Translationen konnte ein signifikanter Effekt auf den medio-lateralen Shift der Patella gezeigt werden. Für eine medio-lateral zentrierte Positionierung des Patellaimplantats auf dem zugehörigen Knochenschnitt konnte eine signifikante Korrelation zwischen dieser Änderung des Patellashifts und dem lateralen Facettenwinkel der nativen Patella gezeigt werden.

Schlussfolgerung und Ausblick

Das neu entwickelte Simulationsmodell liefert valide Ergebnisse für das tibio-femorale Gelenk. Darüber hinaus ermöglicht es qualitative und vergleichende Analysen zwischen verschiedenen Implantat- und Modellkonfigurationen. Um belastbare Aussagen zu Patellakontaktkräften und absoluter patello-femoraler Kinematik machen zu können, sind weitere Validierungsschritte nötig, die zusätzlicher Daten insbesondere zur patello-femoralen Kinematik und Lastsituation bedürfen. Die solide mathematische Grundlage für die Arbeit mit Kinematikdaten aus unterschiedlichen Quellen wurde geschaffen.

Der gezeigte signifikante Zusammenhang zwischen der Beeinflussung des medio-lateralen Shifts durch den Patellarückflächenersatz und dem nativen lateralen Facettenwinkel der Patella kann möglicherweise in der klinischen Anwendung berücksichtigt werden. Die grundlegenden Forschungsergebnisse zur patello-femoralen Kinematik können in zukünftigen Projekten für weitere Validierungsschritte des in dieser Arbeit entwickelten Simulationsmodells genutzt werden. Dies ist insbesondere dann möglich, wenn in naher Zukunft neue Datensätze mit kombinierten Daten zu tibialen in-vivo Lastdaten und patello-femoraler Kinematik verfügbar werden.

2.   Abstract (English):

Background

Anterior knee pain (AKP) is one of the main reasons for patient dissatisfaction after total knee arthroplasty (TKA). Since AKP is localised to the patello-femoral joint and its direct surroundings, it is likely that the causes for AKP are related to this joint. Review of the existing literature on patello-femoral contact forces and patello-femoral wear testing points towards failure-conducing mechanics. This, however, evidently conflicts with the comparably low revision rates reported by several national joint registries for patellar implants. This contradiction highlights the need for an improved understanding of the mechanics of the patello-femoral joint in vivo, as herein may lie the key to successful reduction of AKP after TKA.

Objectives

The first aim of this dissertation was to improve the understanding of the patello-femoral joint by focusing on a new approach to simulate the knee joint. This approach aimed to reduce the dependency of the model on assumptions which are based on non-accurate estimations. In order to validate this model, patello-femoral kinematics need to be further investigated. Therefore, the second aim of this dissertation was to lay the foundation to work with patello-femoral kinematic data with mathematical diligence. Finally, a deeper investigation of the factors influencing patellar kinematics was undertaken by first focusing on analysing the effect of patellar resurfacing in a human donor study.

Materials and Methods

In a first step, a finite element model including the patella was developed based on standardized in vivo load data for the isolated tibio-femoral joint. Since these data implicitly include all forces and moments induced by gravity, dynamics and soft tissue crossing between the proximal and distal segments of the joint, explicit modelling of most of these factors can be avoided without weakening the validity of the model. This model was applied to analyse the effects of the initial proximo-distal patellar position and the stiffness of the patellar tendon on patellar kinematics.

The second part of this dissertation addressed a more fundamental issue, re-establishing solid basic principles with which to analyse and interpret patellar kinematics accurately. The representation of kinematics data, especially of relative patello-femoral rotations, is highly dependent on the underlying mathematical conventions used and their exact execution. A detailed summary of the most common methods to describe patello-femoral ro-

tations was formulated and more importantly, accurate conversions between these conventions were derived. These were provided to the biomechanical research community in the shape of a virtual computation tool.

To improve our understanding of the impact of the parameters which influence patellar kinematics, the effects of patellar resurfacing were isolated from in vitro testing with eight fresh frozen knee specimens on a well-established knee rig at the Musculoskeletal University Center Munich (MUM). To identify the specific effects of patellar resurfacing, knee kinematics were measured both pre- and post-TKA, with and without patellar resurfacing, for two tibio-femoral implant variants (posterior stabilised PS and PS+).

Results

The finite element model made it possible to run comparative studies with different implants or parameter variants. For the tibio-femoral joint, both kinematics and contact loads are in good accordance with the values previously reported in the relevant literature. For the patello-femoral joint, it was shown that a proximal initial patellar position and a weak patellar tendon causes more patello-femoral flexion and spin, while patellar tilt and shift are mainly influenced by the initial patellar position.

The analysis of underlying mathematical conventions on the representation of patello-femoral rotations showed that both magnitude and the characteristics of the rotation curves can be modified fundamentally by switching between conventions. The derived transformation methods between the presented conventions were shown to be valid by way of mathematical proofs and comparison to benchmark data.

In the experimental part of this dissertation, no significant effects of patellar resurfacing on patello-femoral rotations were found. For the translations, it was shown that patellar resurfacing had significant effects on patellar shift. For cases in which the patellar implant was placed in the medio-lateral centre of the patellar cut, this change in patellar shift proved to be significantly correlated to the lateral facet angle of the native patella.

Conclusion and Outlook

The developed model provides valid results for the tibio-femoral joint. Furthermore, it enables qualitative and comparative analyses between different implant and model configurations. Nevertheless, for accurate quantitative results of patellar kinematics and kinetics, additional data for validation are needed, namely in vivo data of patello-femoral kinematics and loads. To handle such kinematic data from different sources, a solid mathematical foundation was established.

The relation shown between the native lateral patellar facet angle and the effect of patellar resurfacing on medio-lateral shift shall be taken into account for clinical applications. In

addition, the basic research on patellar kinematics brought forward by this dissertation can be used in future projects for further validation of the newly developed model, especially once a combined dataset of in vivo tibial loads and patello-femoral kinematic data becomes available.

3.   Introduction

3.1   Motivation and aim

Since total knee arthroplasty (TKA) was in its infancy, the prevalence of anterior knee pain (AKP) after TKA decreased from over 40% in the 1970s to less than 20% today [1–6]. Nevertheless, AKP is still the most common cause for dissatisfaction after TKA [7]. There are numerous possible sources known for AKP like an overloading of soft tissues, impingement or instability [3], but for up to 15% of patients with residual pain no explanation can be found [7].

To fully grasp the implications of patella-related complaints, a comprehensive understanding of knee joint mechanics, especially that of the patello-femoral joint after TKA, is necessary. For the tibio-femoral joint, instrumented implants were placed by two research groups [8–10]. The data collected from these implants have provided crucial knowledge on in vivo mechanics. However, to the best of the author's knowledge, no analogous studies exist where instrumented patellar implants were placed and able to directly measure the contact forces in the patello-femoral joint.

Nevertheless, there are some studies which seek to estimate patello-femoral contact forces. These studies can be divided into three groups. First, there are those which rely on human anatomical specimen data to estimate the contact forces [11–18]. Thereby, in most studies a squat is simulated [11–13,16,17] and more complex activities of daily living, such as level walking are tested rarely [18]. To execute these tests, the body weight is generally reduced to a maximum of one third of its actual value [11–13,16,17]. Scaling the patello-femoral contact forces from such studies with reduced knee loads linearly to real body weights leads to peak patello-femoral contact forces between 3.8 and 8.8 times body weight (BW) for a squat cycle [19]. Although it has been demonstrated that scaling the simulated bodyweight does not change the shape of tibio-femoral kinematic profiles [20], these scaled results for patello-femoral contact forces from human donor specimen tests lead to unrealistically high values. Therefore, linear body weight scaling factors for these force values should be questioned [19].

A second group of studies aiming to quantify patello-femoral contact forces involves analytical calculations based on body movements and forces like ground reaction forces or gravity, which are rudimentary musculoskeletal models. The calculations for these simple models can be executed even without the use of modern computers. As such, these methods were mainly used in older studies and also lead to peak patellar contact forces up to 7.6 BW for a squat [21,22] and 1.36 BW for level walking [23,24].

A third category consists of studies which rely on modern musculoskeletal models and finite element models for the prediction of patello-femoral contact forces. Such more detailed and sophisticated models result in slightly lower contact forces between patella and femur. For a two-legged squat, the patello-femoral contact forces given are in a range between 3.1 BW and 6.0 BW [25–27]. For level walking, stair climbing and sit-to-stand, peak patello-femoral contact forces up to 1.28 BW, 3.53 BW and 4.07 BW, respectively are reported [26,28,29].

Hart et al. [30] pooled nine studies with 152 subjects overall which led to estimates of 0.9 ± 0.4 BW for the peak patello-femoral contact forces during level walking in healthy knees. For stair ascent and descent, they reported 3.2 ± 0.7 BW (6 studies, n=121) and 2.8 ± 0.5 BW (4 studies, n=66), respectively. This consolidated dataset was not restricted to specific methods of measuring or calculating the forces and the final results are in accordance with the previously reported values.

To put these contact forces into perspective, one can refer to the results of prosthetic patello-femoral wear testing [31–35]. Applying loads derived from level walking, with peak patello-femoral contact forces of 1177 N (equivalent to 1.6 BW for a 75 kg person and 1.2 BW for a 100 kg person), the patellar components show significant wear after 3-4 million load cycles [32–34]. For conventional ultra-high-molecular-weight polyethylene (UHMWPE) after gamma sterilisation under vacuum with 25 to 40 kGy (= 2.5 to 4 Mrad) a maximum material loss of 0.95 mm was reported after four million cycles [32]. Since cross-linking of the chains in UHMWPE by higher radiation seemingly increase the wear resistance of the material [36], the conventional UHMWPE was replaced by highly cross-linked UHMWPE (radiation doses ranging from 50 to 100 kGy) in some implants [37]. An in vitro comparison of wear on conventional and highly cross-linked patellar components showed a reduction of subsurface cracks and material loss for the highly cross-linked UHMWPE. Nevertheless, the conventional as well as the highly cross-linked patellar components showed clear scarring and slight plastic deformations after testing five million gait cycles with a peak load of 1750 N. After two million cycles of stair climbing with a peak load of 2468 N (equivalent to 3.4 BW for a 75 kg person and 2.5 BW for a 100 kg person) and well aligned implants, the highly cross-linked patellar component showed wear scars while the conventional component additionally developed subsurface cracks. For a 4° internally malrotated femoral component, the highly cross-linked patellar component showed more severe scarring and deformation while the conventional UHMWPE-component showed substantial material loss at its lateral edge after one million cycles [31]. These in vitro results indicate a higher wear resistance for patellar components made of highly cross-linked UHMWPE.

To evaluate the difference in clinical outcomes between standard and highly cross-linked UHMWPE, registry data were reviewed. Since no registries that discriminate between these two material variants for patellar components were found, revision rates for TKA with tibio-femoral inlays with and without cross-linking were analysed. The Australian Orthopaedic Association National Joint Replacement Registry (AOANJRR) reported that 75.8% of tibio-femoral inlays in TKA in 2021 consisted of cross-linked UHMWPE. Overall, the reported cumulative revision rates for cross-linked UHMWPE are significantly lower than those for conventional UHMWPE [38]. Nevertheless, a deeper look into implant specific data published up until the annual report 2020, revealed inhomogeneous outcomes. For some implant systems cross-linking decreased revision rates, others were unaffected or had higher revision rates using cross-linked UHMWPE [39]. Therefore, the advantage of highly cross-linked UHMWPE that would be expected based on the previously mentioned wear testing of patellar components, was not fully confirmed by registry data.

Overall, previous studies concluded that patellar components show significant wear for loads that are lower than the patellar contact forces described in literature for the tested activities. Additionally, the advantage of highly cross-linked UHMWPE observed in vitro does not show up consistently when analysing implant survival rates. Therefore, the damage on the patellar component in clinical settings could be expected to be more severe than in in vitro wear tests, potentially even leading to implant failure.

Nevertheless, in the national joint registries of Australia, Germany, Great Britain and the United States, cumulative revision rates after TKA are reported to be lower if the patella is resurfaced during the primary surgery. The advantage of TKA with patella resurfacing regarding the revision rates increases over time [38,40,41]. Therefore, it is likely that patellar resurfacing is not causing the additional revision surgeries due to excessive wear of patellar components that one would expect from reviewing the wear testing results and patellar contact force estimations in literature (figure 1).

Therefore, there could be a lack of precise understanding of the mechanics in the knee joint, especially in the patello-femoral joint. Results indicate that current methods may very well be leading to an overestimation of the patello-femoral contact forces. It is precisely this hypothesis which acts as the starting point of this dissertation, opening a broad field of study to dive deeper into the relevant factors and ultimately shed some clarity on the identified conflicting information.
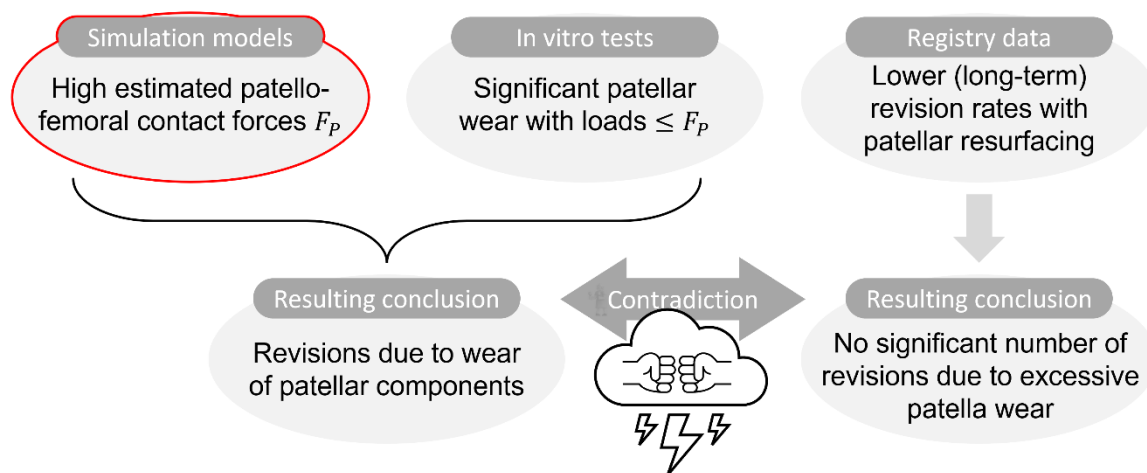
Figure 1: Visual illustration of the starting point for this dissertation. The results of current simulation models and in vitro testing lead to the prediction of artificially high revision rates, conflicting with the lower rates reported by real registry data. This dissertation will focus on a re-exploration of existing simulation models (highlighted in red) as the potential source of this incongruency in the results.

Hence, the aim of this dissertation was to employ newly developed methods to critically assess patello-femoral joint mechanics, ideally identifying the source of this contradiction. To that end, the use of results from in vitro studies, as well as the incorporation of assumptions from existing theoretical investigations, were reduced to a minimum. Since no in vivo data for patello-femoral contact forces are available, the main challenge of this project was and still is to find ways to validate the contact mechanics without using previous force estimations which are questioned in the beginning of this research project. By investigating the causes of the above-mentioned contradictions, the understanding of the patello-femoral joint mechanics is improved. This represents an important basis to further investigate musculoskeletal factors potential to reduce AKP after TKA.

This dissertation consists of three publications. In the first publication, a new dynamic finite element model including the tibio- and patello-femoral joint is presented. The second publication focuses on the theoretical and mathematical foundation of representations of patello-femoral kinematics and how to transform rotational data between these different conventions. In the third publication, the isolated effects of patellar resurfacing on patello-femoral kinematics were extracted from human donor tests to analyse whether patellar resurfacing could potentially lead to changes in kinematics and kinetics that better explain the positive clinical outcomes of patellar implants.

3.2 Finite Element Model

Every biomechanical model demands the consideration of certain assumptions which end up having a notable impact on the results. As a result, the first aim of this dissertation focused on the development of a knee joint model which included the patello-femoral joint,

while keeping the necessary associated assumptions to a minimum. In musculoskeletal models, muscle forces are calculated by optimising a specific criterion. For example, the model may seek to minimise energy consumption [25,42], joint torques [43], maximum relative muscle forces [44], muscle fatigue or the sense of effort [45]. A comparison of some of these criteria showed big differences in the resulting joint reaction forces [44]. Additionally, the exact location of muscle attachments, the respective strength of muscles and specific ligament stiffnesses have notable impacts on the results of such models. Although these parameters can theoretically be determined for each subject specifically, this is not feasible for larger subject populations. To develop a more generalised model, all these parameters would need to be defined based on assumptions which would have a huge impact on the resulting kinetics of the knee joint.

In order to address this, a finite element model was developed that is reduced to an absolute minimum in terms of assumptions using standardised in vivo tibial reaction forces measured by instrumented implants [8,10]. These data consist of three tibio-femoral reaction forces and three tibio-femoral moments representing all loads transmitted via the tibio-femoral contact. All forces induced by ligaments and tendons that cross the tibio-femoral joint line are implicitly included into these loads, as well as forces induced by gravity or gait dynamics. A model where boundary conditions are chosen, such that the tibial reaction moments are equal to the moments from the dataset when the flexion angle and the tibial forces are fed as input will reproduce the in vivo kinematics and contact situation. Following this basic idea, the model described in detail in the **first publication** with the title *"Towards a New, Pre-Clinical, Subject-Independent Test Model for Kinematic Analysis after Total Knee Arthroplasty – Influence of the Proximo-Distal Patella Position and Patellar Tendon Stiffness"* [46] was developed. The strength of this model is its simplicity. Modelling of most ligaments and muscles is avoided by having their effects on the joint implicitly contained in the tibial reaction loads. Only patella-related anatomic elements need to be explicitly modelled. It is useful for pre-clinical testing of implants and for studies comparing some parameters concerning the explicitly modelled patellar component, such as the published effects of the patellar tendon stiffness or the initial position of the patella. For valid estimates of the absolute patello-femoral contact force, the model is not suitable, because these forces are highly dependent on the chosen parameters of the patella integration. Due to the fact that questioning the magnitude of patello-femoral forces in literature was the starting point of this dissertation, such studies should not be used as sources to validate our model. Doing so would inevitably lead to similar results.

Another way to further validate the patella-related results of the model is using more accurate data of patellar kinematics for the validation process. This could be a project for future research that has the potential to bring further insight into the detailed mechanics

of the patello-femoral joint and the foundations for this were laid in the second part of this dissertation.

3.3   Patello-femoral kinematics

A literature search for patello-femoral kinematic data revealed that many publications present kinematic values without properly describing the associated underlying mathematical conventions. Especially in what relates to relative rotations, key information is often missing [47–52]. Without comprehensive descriptions of the used definitions, the data are not uniquely interpretable. Much like providing measurements without the associated units, kinematic data published without clarification of the conventions employed is essentially useless. For kinematic data without clear information on the conventions it is the same type of problem. Another example of the use of questionable conventions is given by Suzuki et al., who reported patello-femoral angles by projecting the patellar axes on femoral planes and calculating the angles between the femoral axes and these projected axes [53]. Although explicitly described and therefore valid in essence, the reader may observe that for increasing patellar flexion angles, the meaning of the reported patellar spin and tilt become increasingly distanced from their clinical interpretations. In fact, for high knee flexion angles, when 90° of patellar flexion are reached, the use of the terms patellar spin and patellar tilt becomes counterintuitive. What one would clinically understand as patellar spin is in fact at this point representing patellar tilt, and vice versa. A similar effect can be observed in cases where patellar flexion is selected as the last rotation of a Cardan sequence, as has also been done in literature [54]. There are some publications proposing exact and clinically meaningful definitions for patello-femoral kinematics, for example Bull et al. [55] who described a convention similar to the mostly used one for the tibio-femoral joint presented by Grood and Suntay [56]. Nevertheless, to the best of the author's knowledge, there has been no publication that provides a comprehensive overview of the possible methods to describe rotation data, as well as their specific advantages and disadvantages. To enable researchers to properly understand the implications of their choice of convention for describing patello-femoral kinematics, such an overview was provided in the **second publication** of this dissertation, titled *"The Influence of Mathematical Definitions on Patellar Kinematics Representations"* [57]. Additionally, methods were developed and implemented to convert numerical data between the common representations for patellar kinematics. An implementation of these conversion algorithms is also given as supplementary material to the publication to facilitate future work with rotational kinematic data. By implementing these methods and, optionally, the accompanying tool, researchers can easily compare results from different studies using different conventions by transforming them into their favoured mathematical definition.

Even when comparing patello-femoral kinematics stemming from a common set of conventions, the associated curves show considerable differences [58,59]. This can be caused by different testing methods, differences between subjects or implant configurations. Therefore, further validation steps for the finite element model with data from literature seem to be critical. In fact, a key goal should be to establish a comprehensive dataset of patello-femoral loads and associated kinematics. Such a dataset is already available for the tibio-femoral joint [60] and as soon as similar data including patello-femoral kinematics is made available, model validation can be moved forward.

Since there are a lot of possible ways to influence the patellar kinematics, there is a need to analyse one of the influencing factors by a time. It was decided to start the exploration of this vast field with an analysis of the effects of patellar resurfacing on patellar kinematics.

Since patellar kinematics differ drastically between subjects [48,61,62], an exceedingly high number of subjects were required to show significant differences between groups with distinct treatment protocols. In order to reach reliable conclusions regarding the effect of varying methods of patellar resurfacing, or even of its omission altogether, a patient cohort of at least 41 to 70 participants would be needed [63–67]. However, if several implant configurations are tested within every specimen, the number of subjects needed to show significant differences decreases to 5 to 10 subjects [68–70]. To avoid problems with interspecimen variabilities, a human specimen study was executed. Eight fresh frozen specimens were tested in a well-established and well understood knee rig at the Musculoskeletal University Center Munich (MUM) [71–78] in their native state. Afterwards, several implant configurations were successively tested, namely, after TKA with posterior stabilised implants (Vega PS and Vega PS+, Aesculap AG, Tuttlingen, Germany), with and without patellar resurfacing. Having the tibio-femoral and patello-femoral kinematic data of every specimen for these five implant configurations enabled to extract the isolated effect of patellar resurfacing on kinematics for the two variants of the Vega implant system. Relating this kinematics analysis back to the native geometry of the patellar bone led to the **third publication**, titled *"Isolated effects of patellar resurfacing in total knee arthroplasty and their relation to native patellar geometry"* [79].

3.4   Conclusion

This dissertation aimed to provide a better understanding of patello-femoral joint mechanics, and thus shed light on the contradiction between the positive clinical results of patellar implants, the in vitro results of wear testing and the published patello-femoral contact force estimates. To that end, a new class of highly simplified models was used to predict patello-

femoral contact forces. In such models, some of the crucial assumptions concerning the soft tissues surrounding the tibio-femoral joint can be bypassed by the use of in vivo load data which implicitly includes this loading. This approach reduces the number of unknowns in the model. For explicitly modelled ligaments and tendons surrounding the patella, the problem cannot be solved without measured in vivo patello-femoral forces. Therefore, validation approaches must be found which do not rely on the values of patello-femoral contact forces reported in literature, as these were questioned at the beginning of this dissertation. One possibility to achieve this aim could be the use of accurate patello-femoral kinematic data. Furthermore, a better understanding of the isolated effects of relevant parameters, such as patellar resurfacing on kinematics, would be enlightening. Within this dissertation, the first steps laying the foundation for this validation process were completed and will act as a useful resource for future projects.

4.   Publication I

Title: Towards a New, Pre-Clinical, Subject-Independent Test Model for Kinematic Analysis after Total Knee Arthroplasty – Influence of the Proximo-Distal Patella Position and Patellar Tendon Stiffness

Authors: Adrian Sauer, Allan Maas, Svenja Ottawa, Alexander Giurea and Thomas M. Grupp

Journal: Journal of applied sciences

Volume: 11

Pages: 1–16

Year: 2021

DOI: https://doi.org/ 10.3390/app112110322

Impact factor: 2.838 (2021)

Article

Towards a New, Pre-Clinical, Subject-Independent Test Model for Kinematic Analysis after Total Knee Arthroplasty—Influence of the Proximo-Distal Patella Position and Patellar Tendon Stiffness

Adrian Sauer [1,2,*] , Allan Maas [1,2] , Svenja Ottawa [1,3], Alexander Giurea [4] and Thomas M. Grupp [1,2]

[1] Research and Development, Aesculap AG, 78532 Tuttlingen, Germany; Allan.Maas@aesculap.de (A.M.); svenja.ottawa@aesculap.de (S.O.); thomas.grupp@aesculap.de (T.M.G.)
[2] Department of Orthopaedic and Trauma Surgery, Musculoskeletal University Center Munich (MUM), Campus Grosshadern, Ludwig Maximilians University Munich, 81377 Munich, Germany
[3] Faculty of Industrial Technologies, Campus Tuttlingen, University of Furtwangen, 78532 Tuttlingen, Germany
[4] Department of Orthopaedic Surgery, Medical University of Vienna, Waehringer Guertel 18–20, 1090 Vienna, Austria; a.giurea@gmx.at
[*] Correspondence: Adrian.Sauer@aesculap.de

Featured Application: This new framework for simulating the knee after total knee arthroplasty is intended to facilitate kinematic analyses in implant development processes and analyses of effects of various individual anatomic properties.

Abstract: Although simulation models are heavily used in biomechanical research and testing of TKA implants, pre-clinical tools for a holistic estimation of implant performance under dynamic loading conditions are rare. The objective of this study was the development of an efficient pre-clinical test method for analyzing knee contact mechanics and kinematics based on a dynamic FE model and to evaluate the effects of the proximo-distal patella position and the patellar tendon stiffness on the patellar kinematics. A finite element-based workflow for knee prostheses designs was developed based on standardized in vivo load data, which included the tibial forces and moments. In a new research approach, the tibial forces are used as input for the model, whereas the tibial moments were used to validate the results. For the standardized sit down, stand up, and knee bend load cycles, the calculated tibial moments show only small deviations from the reference values—especially for high flexion angles. For the knee bend cycle, the maximum absolute value of patellar flexion decreases for higher patellar tendon stiffness and more distally placed patellar components. Therefore, patella-related clinical problems caused by patella baja may also arise if the patellar tendon is too weak for high tibiofemoral flexion angles.

Keywords: dynamic finite element model; knee kinematics; patellofemoral kinematics; pre-clinical testing; total knee arthroplasty; patellar tendon; patella alta; patella baja

1. Introduction

Total knee arthroplasty (TKA) is a prevalent treatment option for osteoarthritis [1], which is the indication for 88% of TKA surgeries [2]. Ten years after surgery, survival rates are 86.1–93.8% [3–8] and satisfaction rates are 81%. This means 19% of patients are either dissatisfied with or uncertain about the results of their procedure [9]. The rate of revisions due to aseptic causes in the first 15 years after primary TKA is 3% [10].

The detection and elimination of implant-related issues that may lead to clinical problems once the implant system is marketed is the main focus of the pre-clinical testing phase. Aside from continuous biomechanical research, there are additional mandatory steps for implant manufacturers. To achieve regulatory clearance, standardized tests need

to be performed in the pre-clinical testing stage. The majority of these tests focus on single components under high cyclic [11–13] or static [14] loading conditions. Pre-clinical test methods under physiological loading conditions (e.g., simulation of daily living activities in a tribological wear simulator [15–19]) exist and enable more complex assessments, such as the analysis of the resulting knee kinematics with an implant.

However, running these tests is time-consuming and cost-intensive [20]. Hence, they are usually only executed towards the end of the design process, with only the final design or with very few design variants in a single size combination.

To analyze knee kinematics and possible biomechanical causes for unmet patient expectations after TKA, computational simulation of joint mechanics is frequently used [21–26]. The state of the art in biomechanical research to precisely predict the kinematics for one specific combination of implant design and subject are musculoskeletal models [27]. However, the great effort needed to adapt such musculoskeletal models to several design variants or size combinations prevents their routine use in early stages of implant design. On the other hand, there are only a few FE models published that are suitable for kinematic analyses [28,29].

To the best of our knowledge, there are no models available with the ability to compare multifarious implant designs and size combinations concerning kinematics and implant loads without massive effort for every single variation. With such a model, it would be possible to identify the combination of design parameters which leads to the best possible fit to the defined requirements [30].

This work is part of a project which aims to address this lack of dynamic FE models of the knee joint for design stage and pre-clinical testing of new prostheses. The newly developed model is intended to be a tool to compare implant loading, component stresses, and kinematic behavior of the tibiofemoral and the patellofemoral joint for various implant design variants or for variations of other parameters, such as the stiffness of the patellar tendon or any other ligaments. In this model, only standardized tibial loads and flexion angles [31] are needed as an input, and the relative kinematics are part of the results.

To be able to run meaningful parametrical studies to improve implant designs, the model should be fast to solve without compromising the informative value of the dynamic results. In accordance with all standardized testing scenarios, the influence of effects caused by individual patient parameters needs to be restrained in order to achieve comparable results.

Besides the possibility to analyze effects of implant design changes, this model is also intended to uncover effects of changes in the explicitly modeled anatomical structures. This will be shown within this study by analyzing the effects of varying patellar tendon stiffness and initial proximo-distal position of the patella on patellar kinematics.

2. Materials and Methods

Standardized loads from eight subjects undergoing total knee arthroplasty with instrumented implants were used as basis for this analysis. These loads are scaled to a bodyweight (BW) of 100 kg [31,32]. The three tibial force and moment components are given in a tibia-fixed coordinate system. In the simulation, the same coordinates are used. The x-, y-, and z-axes are directed laterally, anteriorly, and proximally, respectively, and the origin is placed halfway between the deepest points of the gliding surface of the polyethylene (PE) insert (Figure 1).
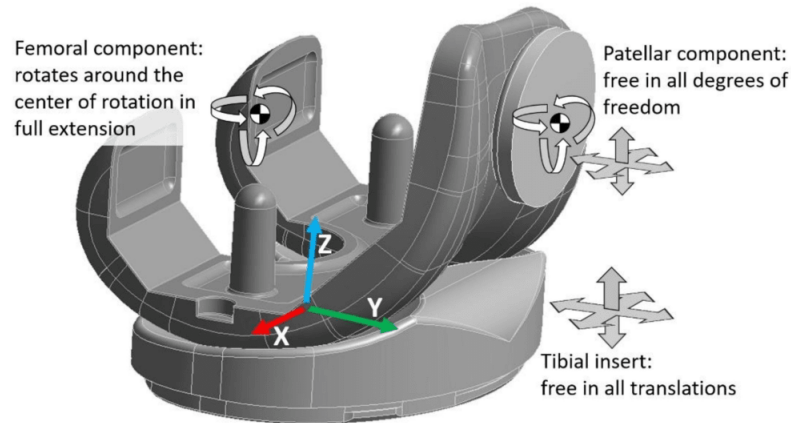
Figure 1. CAD model of the used implant components and the global coordinate system.

2.1. Concept and Assumptions

The central hypothesis for this model is that, in combination with the given tibial forces, only the real knee joint kinematics, especially the correct tibiofemoral contact situation, will lead to the given tibial reaction moment. Only the tibial forces and the flexion angle given by the dataset were used as input data to enable the validation of the FE-simulation results. The corresponding moments are then compared to the reaction moments output by the simulation.

In order to take the patella into account, the model must be adjusted such that the proportion of tibial forces caused by ground reaction forces are separated from the forces caused by muscles and ligaments. Without additional information regarding the direction and magnitude of ground reaction forces, it is not possible to achieve this reliably for load cycles with highly dynamic ground reaction forces. Therefore, two fundamentally different models were developed. The first includes the patella for the knee bend, sit down, and stand up cycles, and the second can handle all load cycles but does not contain any patella-related information. This paper presents only the first model, which includes the patella.

By using the standardized loads given by Bergmann et al. [31], patient-individual effects were reduced. These patient-individual effects were further reduced by avoiding individual bone geometries in the model. In this simulation, there was no need to consider bones and most muscles and ligaments because their impact is implied by the load data. Bergmann et al. [31] used the Zimmer Innex system (Zimmer Biomet, Warsaw, Indiana) for their measurements, a highly congruent, cruciate-sacrificing, and fixed-bearing implant. The properties of fixed-bearing tibial components allow the tibial implant component to be replaced by boundary conditions for the PE insert. Therefore, this model was reduced to the femoral component, the PE insert, and the patella component (Figure 1). Because the original implant geometry used in the study of Bergmann et al. [31] was not available, a comparable design (Columbus UC, Aesculap AG, Tuttlingen, Germany) and size combination (PE insert size 4, femur size 4, and patella size 1) was used.

2.2. FE Model

The six degrees of freedom between femoral and tibial implant component were defined as follows (Figure 1): The femoral component was free to revolve around a fixed center of rotation, which coincided with the center of rotation in full extension. The tibial component was free to translate in all axes with fixed rotations. The separation of translational and rotational degrees of freedom of the tibiofemoral joint in the described way led to a stable FE model without restricting the relative kinematics in any way. The flexion

angle was the only degree of freedom, which was predefined by the dataset. So, there remain five degrees of freedom according to the tibiofemoral kinematics. The patella has six additional degrees of freedom and is only guided by its contact to the trochlear groove and four spring-elements, which modeled the function of the patellar and quadriceps tendons (Figures 1 and 2).
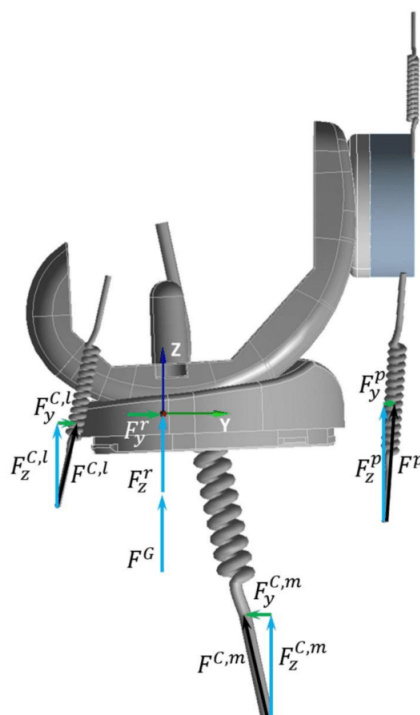

Figure 2. Tibial forces (black) and their components in *y* (green)- and *z* (blue)-directions, respectively.

There are two main contact areas in the knee joint which had to be taken into account. Both the tibiofemoral and the patellofemoral contact areas were modeled as asymmetric augmented Lagrangian contacts. A coefficient of friction of 0.05 was used for this simulation [33–35].

To minimize computing time, the small deformation of the femoral component was neglected, and it was instead defined as rigid body. Therefore, only some contact elements on its surface were needed, instead of a fully meshed geometry [36–38]. The material properties of the PE insert and the patella component were defined by a bilinear stress–strain curve with a yield strength of 25 MPa [33].

In the first step of the calculation, the flexion angle and the standardized tibial forces F_x^B, F_y^B, and F_z^B in the lateral (*x*-axis), anterior (*y*-axis), and proximal (*z*-axis) directions, as given by Bergmann et al. [31], were used as time-dependent input. Secondary input data were calculated from this primary data and provided as input for the FE model. The flexion angle was the only degree of freedom which was externally controlled. The given tibial forces could not directly be applied to the PE insert because the forces acting on the patellar tendon (F^P) and collateral ligaments (medial: $F^{C,m}$ and lateral: $F^{C,l}$) and the ground reaction forces (F^G) had to be subtracted first. In this study, the upper indices identified the forces or moments, while lower indices specified components of vectorial variables.

Forces caused by tissues, muscles, and ligaments, which are not explicitly modeled, are summarized by an additional force vector F^r. It complements the explicit modeled forces acting on the tibia to the standardized tibial loads F^B. This simplification allows

to avoid the modeling of every single muscle and ligament, which would exceed the acceptable effort in modeling and solving for an everyday design evaluation tool without providing better results regarding implant loads and kinematics.

For the ground reaction force, 490.5 N (100 kg BW divided by two legs) are applied normal to the plane of the tibial plateau. Figure 2 shows the described forces with their components in the *y*- and *z*-directions. In a frontal view, the same could be performed for the *x*- and *z*-directions.

To split the standardized loads into the single forces stated above, the equilibrium of forces in the proximal (*z*) and anterior (*y*) directions from a sagittal view is set up. The described forces must replace the forces from the load data, which led to

$$F_z^B = F^G + F_z^r + F_z^P + F_z^{C,m} + F_z^{C,l} \text{ and} \tag{1}$$

$$F_y^B = F_y^r + F_y^P + F_y^{C,m} + F_y^{C,l} \tag{2}$$

The angle of the patellar tendon is used to derive the equation for F_y^P from F_z^P, which results from Equation (1). Finally, Equation (2) gives the residual forces in the anterior direction. The described precalculation in the sagittal plane only considered forces acting parallel to this plane.

The forces of the collateral ligaments are initialized using their positions at full extension. Its *z*-components are calculated under the assumption that the patellar tendon force is zero. Therefore, an initial force distribution of 55% medial and 45% lateral is used, based on their ratio of ultimate tensile strength [39]. As shown in Figure 3, the same equation could be used to calculate the *z*-component of the patella tendon force for subsequent time steps by using the collateral ligament forces $F^{C,m}$ and $F^{C,l}$ calculated from kinematic results of previous simulation runs. By using the angle of the patellar tendon given by previous simulation runs, the total patellar–tendon force could be obtained, as well as its *y*-component, which is needed to calculate F_y^r using Equation (2). The calculation of F_x^r was analogous to the described algorithm for F_y^r.
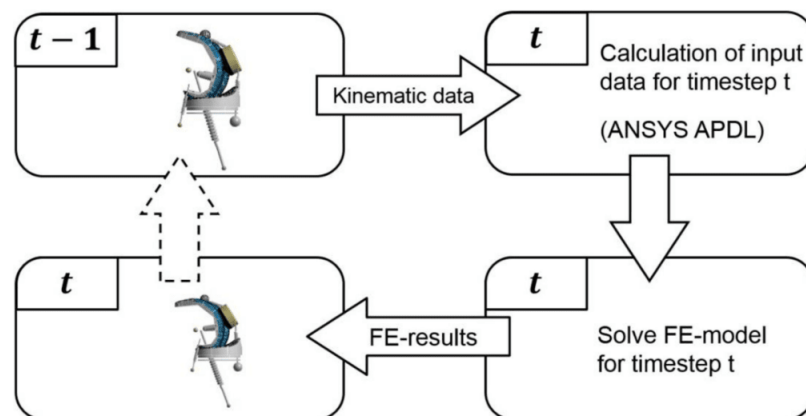

Figure 3. Iterative solving process using kinematic data from previous time step.

As per Wilson et al. [39], who reported no significant difference between medial and lateral collateral ligament, the stiffness of the collateral ligaments was set to 60 N/mm. The four studies in this review, which used moderate elongation rates ($\leq$200 mm/min), reported an averaged stiffness between 58 and 65 N/mm [40–43].

To be able to consider the forces of the collateral ligaments when calculating the input data for the FE model, it was necessary to calculate their length using kinematic data from previous results. Therefore, the simulation was divided into 600 steps, one for every

period between two data points in the given dataset from Bergmann et al. [31]. To calculate the input data (F_x^r, F_y^r, and F_z^r) for time step t, the kinematic results from step $t-1$ were used. The deviation in tibial forces, which was caused by the delay of one time step of the kinematic data for calculating the input data, was negligible.

To implement the described algorithm, Ansys Workbench (Release 19.2) and Ansys Mechanical APDL were used. Inertial forces of the simulated components have only minor effects on this analysis because the simulated load cycles do not contain high accelerations and can be assumed as quasi-static. The small inertial forces of the body are implicitly included by using input data from instrumented implants. Nevertheless, to achieve a high numerical stability, a full transient analysis type using a sparse matrix direct solver was chosen in this study.

The tibial moments are given within the reference frame shown in Figure 1, and the tibiofemoral kinematics given in this study are defined as follows: the flexion angle is given as relative rotation of the femoral to the tibial component around the femoral medio-lateral axis of the implant. A positive femoral anterior–posterior translation (AP translation) is given as femoral movement to posterior parallel to the tibial y-axis, which is shown in Figure 1. The femoral rotation is the rotation of the femoral component around the tibial proximo-distal axis. Medial rotation is defined to be positive.

The patellar kinematics are given as relative movements of the patella with respect to the femoral coordinate system, as shown in Figure 4. The rotations are calculated as cardan sequence using the rotation order flexion–spin–tilt. Therefore, the patellar flexion is given as the relative rotation of the patella with respect to the femur around the femoral flexion axis. The values are negative if the patella flexes less than the femur, which is usually the case. The patellar tilt is described as the rotation around the patellar proximo-distal axis, with a positive sign if the patella rotates towards the medial side. For patellar spin, the axis is given as floating axis orthogonal to the other two. If the patellar spin is positive, then the proximal tip of the patella rotates towards the lateral side.
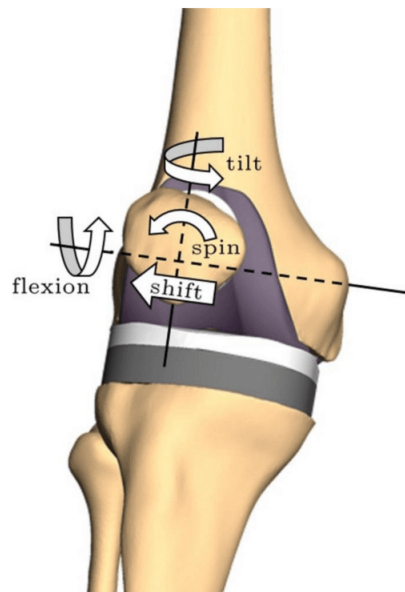

Figure 4. Patellar rotations and patellar shift. Shift along, and flexion around, femoral flexion axis, tilt around patellar proximo-distal axis, and spin around a floating axis orthogonal to the first two axes. Arrows are pointing to positive directions (basic image for this figure from model presented in [27]).

A positive patellar shift is given as relative movement of the center point of the patella with respect to the femur in the lateral direction along the femoral flexion axis. All kinematics data are measured relative to their neutral position in full extension.

3. Results

The tibial reaction moments are the main results for the validation of the described model. The comparison between simulation results and the reference values from literature is shown in Figure 5 for the load cycles corresponding to knee bend, sit down, and stand up.
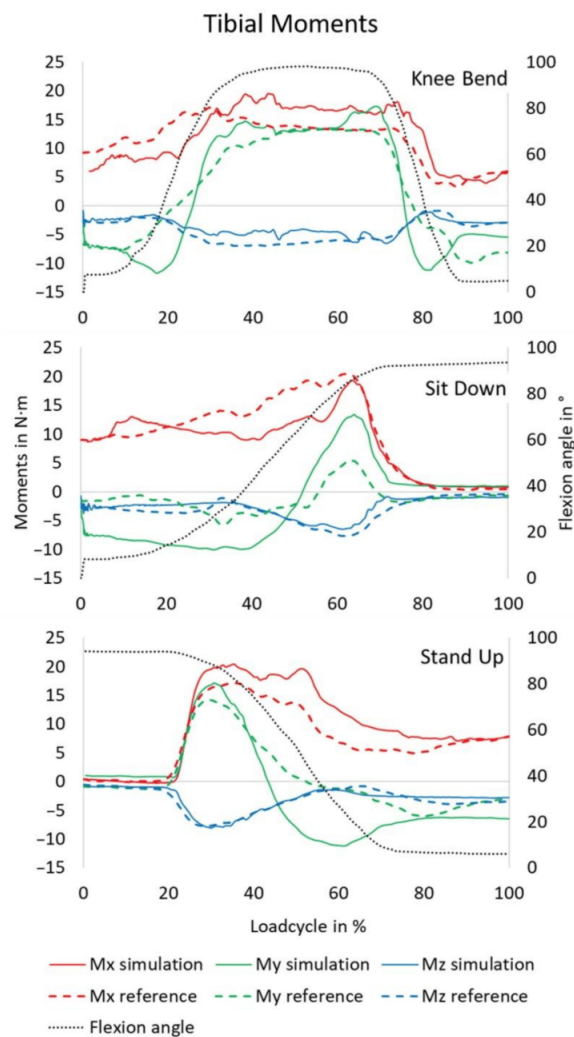
Figure 5. Comparison of simulation output to the reference data for the tibial moments for knee bend, sit down, and stand up cycles.

During weight-bearing squat, the medial tibial contact force was higher than the lateral one for low flexion angles. They showed equal values of 1350 N at the point of the zero-crossing of the varus–valgus moment at $75°$ of flexion. For higher flexion angles, the lateral contact force was the dominant one. At $30°$ ($60°$, $90°$) of flexion, the medial and lateral tibial contact forces reached 999 N (1310 N, 1373 N) and 478 N (950 N, 1700 N).

At the point of the maximum resultant tibial contact forces, the proportion of the medial contact force was 40% of the total tibial contact forces. Figure 6 shows the medial and lateral tibial contact forces for all three load cycles.
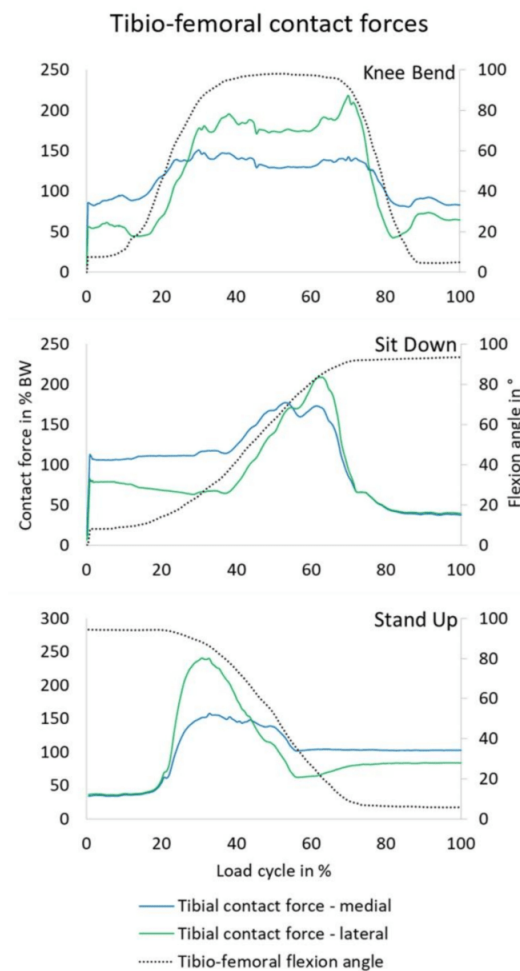
Figure 6. Tibial contact forces in medial and lateral compartment during weight-bearing squat.

For the knee bend cycle, the peak patellofemoral force was reached during the upwards movement at 91.4° of flexion with a magnitude of 2563 N, which is equal to 2.61 BW. The sit down cycle (stand up cycle) led to a maximum patellofemoral force of 2600 N/2.65 BW (2872 N/2.93 BW) at 84.2° (86.1°) of flexion.

The main translational and rotational degrees of freedom, which are femoral AP translation and tibial rotation around its axis, were analyzed and are shown in Figure 7. The mean relative femoral AP translation was equal to the tibial translation in the opposite direction, which was directly given by the model. For the 98° squat, the maximum AP translation between femur and tibia was 16 mm at a flexion angle of 98.1°.
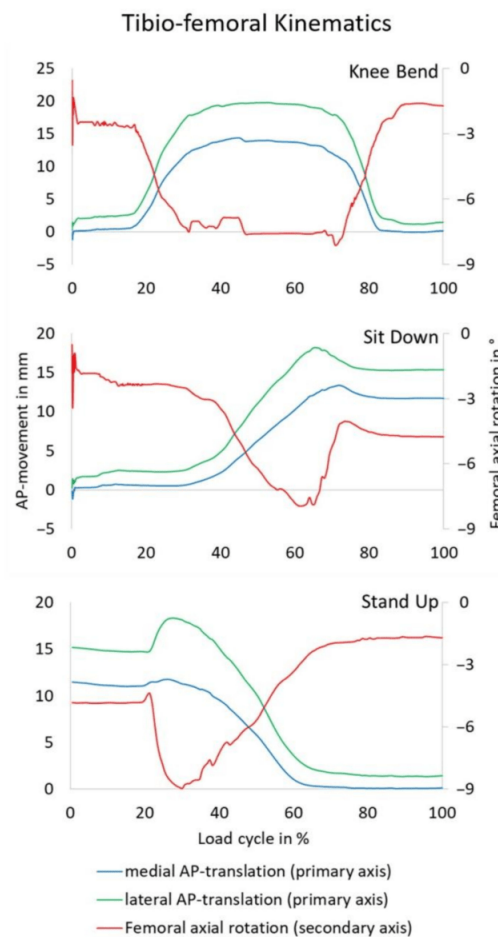
Figure 7. Femoral rollback of medial and lateral condyle and the axial femoral rotation for sit down, stand up, and knee bend cycle.

The tibial rotation could also be directly derived from this model by taking the femoral rotation around the tibial z-axis with a negative sign (Figure 7). A maximum tibial rotation of 8° was calculated at 93.6° of flexion (knee bend cycle).

For applications without evaluation of the tibiofemoral contact, the PE insert could be simulated as a rigid body to decrease computational time by about 10% without changing kinematics in a considerable way. The averaged difference between the curves of the tibial reaction moments was less than 4%. Furthermore, taking peak patellofemoral force during the knee bend cycle as an example, this value changed by only 42 N, going from 2539 N to 2581 N when simulating the PE insert as a rigid body.

The patellar kinematics were analyzed under variations of the patellar tendon stiffness between 300 N/mm and 1000 N/mm, and the initial proximo-distal patellar position was simultaneously varied in a range of ±6 mm.

The peak values of patellar flexion, spin, and tilt during the downwards movement of the knee bend are given in Figures 8–10. The maximum absolute values of patellar flexion decrease for a decreasing stiffness of the patellar tendon and for a more proximally-placed patella. The peak values of patellar spin are between 3.64° and 5.26° of lateral rotation.

The patellar spin increases with a weaker patellar tendon and for patellae placed more proximally. The range of peak values of patellar tilt is between 3.35° and 3.68° of medial tilt and no clear relationship to the initial patellar proximo-distal position or the stiffness of the patellar tendon can be seen.
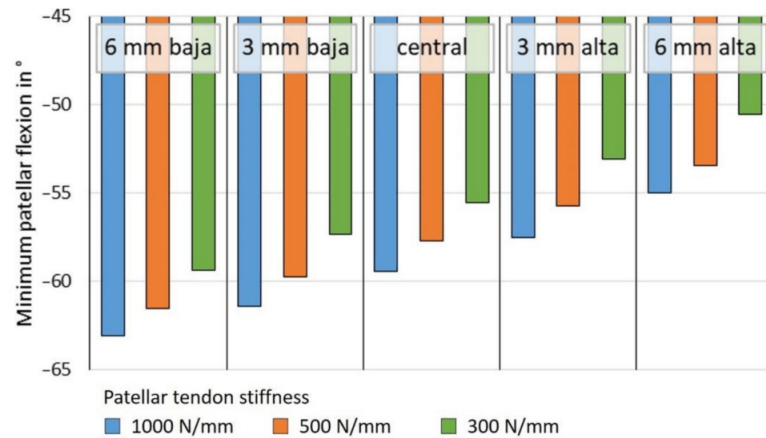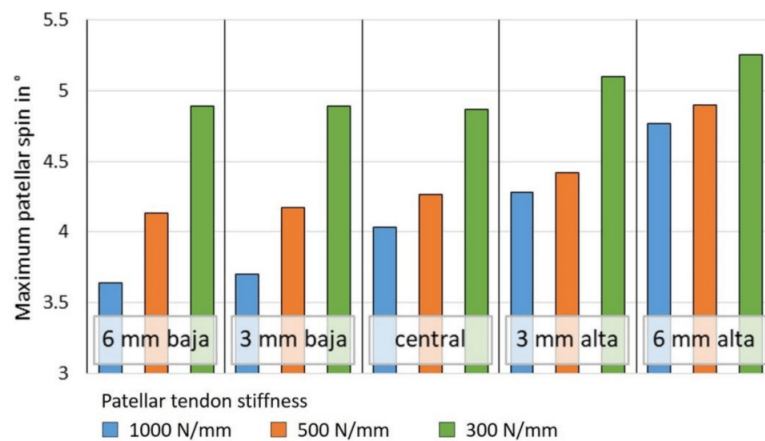

Figure 8. Peak values of the patellar flexion during weight-bearing squat for several initial patellar positions (left to right: 6 mm baja to 6 mm alta) and patellar tendon stiffnesses (blue: 1000 N/mm, orange: 500 N/mm, and green: 300 N/mm). Flexion is given around the femoral flexion axis relative to the femoral implant component. Negative values indicate that the patella flexes less than the femur.

Figure 9. Peak values of the patellar spin during weight-bearing squat for several initial patellar positions (left to right: 6 mm baja to 6 mm alta) and patellar tendon stiffnesses (blue: 1000 N/mm, orange: 500 N/mm, and green: 300 N/mm). Spin is given as rotation around the floating axis between the femoral flexion axis and the patellar proximo-distal axis. A positive sign indicates a rotation to lateral direction.
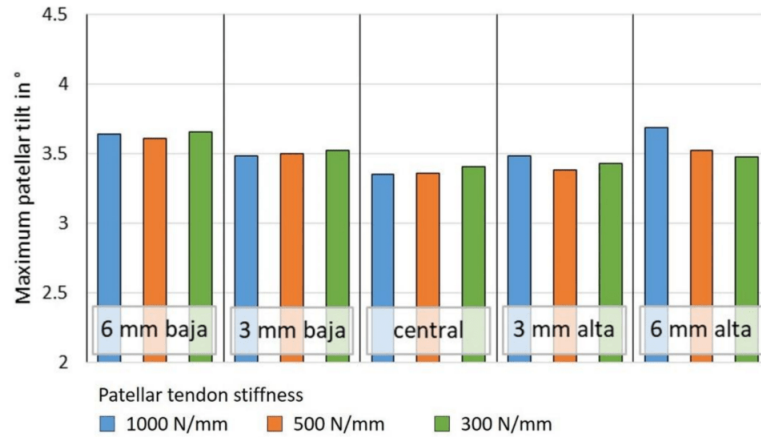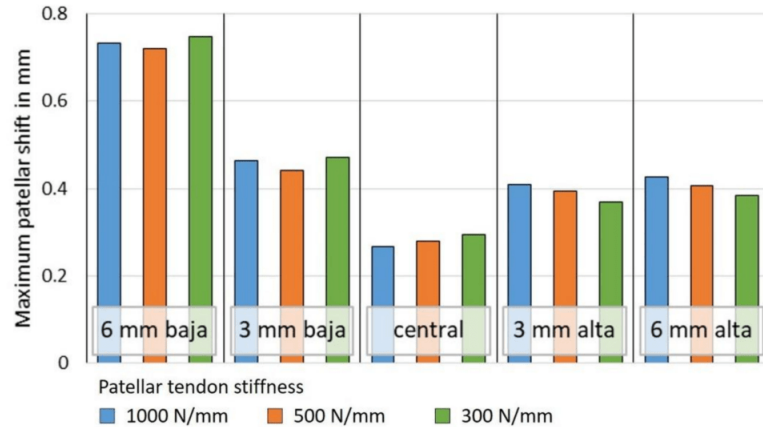
Figure 10. Peak values of the patellar tilt during weight-bearing squat for several initial patellar positions (left to right: 6 mm baja to 6 mm alta) and patellar tendon stiffnesses (blue: 1000 N/mm, orange: 500 N/mm, and green: 300 N/mm). Patellar tilt is given as rotation around the patellar proximo-distal axis. Rotations of the patella to the medial side have a positive sign.

The peaks of the patellar shift shown in Figure 11 are between 0.27 mm and 0.75 mm to the medial side. While the initial proximo-distal position of the patella influences the peak patellar shift, the stiffness of the patellar tendon has only minor effects on the patellar shift.

Figure 11. Peak values of the patellar shift during weight-bearing squat for several initial patellar positions (left to right: 6 mm baja to 6 mm alta) and patellar tendon stiffnesses (blue: 1000 N/mm, orange: 500 N/mm, and green: 300 N/mm). A positive patellar shift is given for relative patellar movements along the femoral mediolateral axis in lateral direction.

Depending on the question that is addressed with this framework, solution times vary from 50 min in a rigid body setup, to determine moment reactions and resulting kinematics, to 4 h when detailed results of the contact situation of a flexible PE component are needed with a high mesh density and element sizes down to 0.75 mm.

4. Discussion

The objective of this study was to develop a dynamic FE model for pre-clinical analysis of knee contact mechanics and kinematics based on standardized loading conditions and to

analyze the effects of various changes of anatomic properties of a knee, such as the patellar tendon stiffness or the proximo-distal position of the patella. This model was intended to be used to analyze multifarious design variants during the implant design and pre-clinical testing process using a fast and straightforward workflow. Therefore, it should be fast to adapt and solve.

The reduced complexity of the model was achieved by partially replacing tissues and bone geometries by boundary conditions. Therefore, the informative value of the results was limited to implant kinematics, loads, and stresses. Findings according to the specific behavior of soft tissue structures surrounding the knee were limited to the explicitly modeled structures, such as the patellar tendon. However, established pre-clinical testing methods are either based on nonstandardized data (e.g., [44,45]) or neglect soft tissue structures and other patient-specific parameters (e.g., [18]). Therefore, the limitation that only the effects of some soft tissue structures can be analyzed turns into an advantage relative to other established standardized pre-clinical testing methods.

Another limitation may arise by the fact that implant geometries were used, which were slightly different from the implants used to create the standardized loads [31]. However, Freed et al. [46] compared the axial tibial loads from measurements and a numeric model with the standardized loads, and even though they used a different ultra-congruent cruciate sacrificing implant than Bergmann et al. [31], there were no significant differences for the quasi-static load cycles of sitting down and rising from a chair. These load cycles are similar to the knee bend cycle, which was also used in our study. Therefore, it is assumed that the use of the implant components of Columbus® UC did not cause substantial differences.

The remaining data from the given dataset, which were not used as input for the simulation, could be used to evaluate the simulation results. The moment around the flexion axis (M_x) and the varus–valgus moment (M_y) were in good accordance with deep flexion angles, and a deviation could be seen in extension. Regarding the moment around the tibial axis (M_z), the simulation results were also consistent with the dataset from literature for small flexion angles. As shown in Figure 5, all of the curves show characteristics which are similar to the standardized load data. Therefore, the model seems to be reliable according to tibial moments and forces, especially for deeper flexion angles, which are more relevant and critical to simulate.

The contact forces in the tibial condyles were compared to an analysis of Kutzner et al. [47], who calculated the medial force ratios from nine patients for different daily activities. Some of their patients were also in the patient cohort for the standardized loads [31], which were used in the present study. If the different level of the total resulting forces is considered, the curves of medial and lateral tibial contact forces are similar for the present study compared to Kutzner et al. [47]. The medial force ratio in the tibia was 40% at the instant of maximum total contact forces, which fits well to the 42% ± 8% which were given by Kutzner et al. [47]. The varus–valgus moment is changing its sign from negative to positive at 75° of flexion during knee bend. This results in a switch of the dominant tibiofemoral contact force from the medial to the lateral condyle, as shown in Figure 6. Therefore, the most loaded condyle in a deep knee bend cycle is the lateral one. At first glance, this might be inconsistent with the fact that in most patients, the medial condyle is more affected by osteoarthritis than the lateral one [48] and 90–95% of unicompartmental knee arthroplasties are placed on the medial side [49]. A deeper look into data from instrumented knee implants [31] shows positive varus–valgus moments mainly for deep flexion angles in symmetric two-legged load cycles, such as knee bend, sit down, and stand up from a chair. The lower relative prevalence of these cycles, compared to level walking, stairs up, and stairs down cycles, with high negative varus–valgus moments explain the higher risk of osteoarthritis on the medial condyle. For the sit down and stand up cycles, the results are also in good agreement with the given data from Kutzner et al. [47].

For two of the eight patients that were included into the standardized loads from Bergmann et al. [31], a subject-specific calculation was made by Trepczynski et al. [50].

They calculated 3.2 BW as averaged peak patellofemoral contact force during a squat at a flexion angle of 94°. Their results for the two patients were 2.6 BW and 3.7 BW. The maximum of 2.6 BW for the patella contact force at 91.4° of flexion that was detected in the present study is equal to the lower bound of the study stated above. Research from other groups, with different patient cohorts, showed patellofemoral forces for a squat at 100° of flexion in a range of 2.7 BW to 3.5 BW [51,52].

Compared to the given literature values, the results of the herein described simulation approach show good agreement, especially for high flexion angles, where the most critical loads are reached. Therefore, the model demonstrates potential to be a useful tool to evaluate implant designs in a platform development approach of new knee systems. It is possible to fully automate the simulation process, which makes it possible to test a great number of geometries in an efficient way. To improve the model, additional validation steps can be performed in future with the CAMS-Knee dataset. This dataset contains tibial loads and kinematics data measured by video fluoroscopy [53].

Further development of this methodology can enable implant manufacturers to achieve more realistic kinematic behavior on a systematic scale by considering dynamic loading and tibio- and patellofemoral kinematics, as well as contact mechanics in a standardized workflow.

Especially in combination with a second model, which will be able to handle load cycles with dynamic ground reaction forces but dispenses with considering the patella, this method opens a wide field of subjects to investigate in an efficient way—from effects of design changes in patellar and trochlear geometries to the impact of different alignment methods.

The analysis of patellar kinematics shows the effects of proximo-distal patellar position and patellar tendon stiffness. According to patellar flexion, both patella baja and high patellar tendon stiffness lead to an increase in relative patellar flexion angles. Therefore, problems occurring in knees with patella baja for high flexion angles could also occur in knees with a central patellar position and a very strong patellar tendon. A weak patellar tendon also increases patellar spin and has minor effects on patellar tilt and shift. The proximo-distal position of the patella is the main parameter to determine the patellar tilt and shift. Both have their minimum for a central patella and increase for patella baja and alta, where the effect is stronger for the patella baja. The changes in the peak values for shift and tilt are very small, with a maximum difference of 0.27 mm and 0.33°. Therefore, the effects of the proximo-distal position of the patella and the patellar tendon stiffness on shift and tilt seem to have only minor clinical relevance.

A patella baja can lead to impingement, anterior knee pain, and a reduced range of motion [54,55]. Consequently, the described changes in patellar kinematics may have an impact on TKA performance and satisfaction in patients with patella baja.

5. Conclusions

A new approach for FE analysis of the knee contact mechanics and kinematics after TKA, which allows to compare multifarious design variants in an efficient way, is presented. As input data, standardized loads for knee bend, sit down, and stand up cycles were used. Some elements of these datasets were used to validate the model.

Due to the use of data based on measurements of instrumented tibial implants, only a few ligament and muscle forces had to be modeled explicitly. The remaining tissues were implicitly contained into the tibial forces used as input. This way of reducing the complexity of the model led to an easy to handle model, which can be solved fast. This model is suitable for the intended use of pre-clinical screening of many design variants, unlike many common pre-clinical testing models, which are mostly static and therefore not suitable to analyze kinematic properties of implant designs.

The presented model is additionally capable to analyze effects of various parameters, such as implant positions or properties of the explicitly modeled ligaments such as patellar tendon stiffness. By varying these two parameters, this study showed that changes of the

patellar tendon stiffness have very similar effects on patellar flexion for high tibiofemoral flexion angles. Therefore, clinical issues related to patella baja or alta in deep tibiofemoral flexion could also be caused by changes in patellar tendon stiffness for normal proximo-distal position of the patella in extension.

References

1. Rönn, K.; Reischl, N.; Gautier, E.; Jacobi, M. Current surgical treatment of knee osteoarthritis. *Arthritis* **2011**, *2011*, 454873. [CrossRef]
2. Robertsson, O.; Bizjajeva, S.; Fenstad, A.M.; Furnes, O.; Lidgren, L.; Mehnert, F.; Odgaard, A.; Pedersen, A.B.; Havelin, L.I. Knee arthroplasty in Denmark, Norway and Sweden. A pilot study from the Nordic Arthroplasty Register Association. *Acta Orthop.* **2010**, *81*, 82–89. [CrossRef]
3. Bae, D.K.; Song, S.J.; Heo, D.B.; Lee, S.H.; Song, W.J. Long-term survival rate of implants and modes of failure after revision total knee arthroplasty by a single surgeon. *J. Arthroplast.* **2013**, *28*, 1130–1134. [CrossRef]
4. Argenson, J.-N.; Boisgard, S.; Parratte, S.; Descamps, S.; Bercovy, M.; Bonnevialle, P.; Briard, J.-L.; Brilhault, J.; Chouteau, J.; Nizard, R.; et al. Survival analysis of total knee arthroplasty at a minimum 10 years' follow-up: A multicenter French nationwide study including 846 cases. *Orthop. Traumatol. Surg. Res.* **2013**, *99*, 385–390. [CrossRef]
5. Bae, D.K.; Song, S.J.; Park, M.J.; Eoh, J.H.; Song, J.H.; Park, C.H. Twenty-year survival analysis in total knee arthroplasty by a single surgeon. *J. Arthroplast.* **2012**, *27*, 1297–1304. [CrossRef] [PubMed]
6. Koskinen, E.; Eskelinen, A.; Paavolainen, P.; Pulkkinen, P.; Remes, V. Comparison of survival and cost-effectiveness between unicondylar arthroplasty and total knee arthroplasty in patients with primary osteoarthritis: A follow-up study of 50,493 knee replacements from the Finnish Arthroplasty Register. *Acta Orthop.* **2008**, *79*, 499–507. [CrossRef] [PubMed]
7. Labek, G.; Thaler, M.; Janda, W.; Agreiter, M.; Stöckl, B. Revision rates after total joint replacement: Cumulative results from worldwide joint register datasets. *J. Bone Jt. Surg. Br.* **2011**, *93*, 293–297. [CrossRef] [PubMed]
8. Sadoghi, P.; Liebensteiner, M.; Agreiter, M.; Leithner, A.; Böhler, N.; Labek, G. Revision surgery after total joint arthroplasty: A complication-based analysis using worldwide arthroplasty registers. *J. Arthroplast.* **2013**, *28*, 1329–1332. [CrossRef]
9. Robertsson, O.; Dunbar, M.; Pehrsson, T.; Knutson, K.; Lidgren, L. Patient satisfaction after knee arthroplasty: A report on 27,372 knees operated on between 1981 and 1995 in Sweden. *Acta Orthop. Scand.* **2000**, *71*, 262–267. [CrossRef]
10. Jorgensen, N.B.; McAuliffe, M.; Orschulok, T.; Lorimer, M.F.; de Steiger, R. Major Aseptic Revision Following Total Knee Replacement: A Study of 478,081 Total Knee Replacements from the Australian Orthopaedic Association National Joint Replacement Registry. *J. Bone Jt. Surg. Am.* **2019**, *101*, 302–310. [CrossRef]
11. ASTM F2723-13a. *Standard Test Method for Evaluating Mobile Bearing Knee Tibial Baseplate/Bearing Resistance to Dynamic Disassociation*; ASTM International: West Conshohocken, PA, USA, 2013.
12. ASTM F2722-15. *Standard Practice for Evaluating Mobile Bearing Knee Tibial Baseplate Rotational Stops*; ASTM International: West Conshohocken, PA, USA, 2015.

13. ASTM F2777-16. *Standard Test Method for Evaluating Knee Bearing (Tibial Insert) Endurance and Deformation Under High Flexion*; ASTM International: West Conshohocken, PA, USA, 2016.
14. ASTM F2083-12. *Standard Specification for Knee Replacement Prosthesis*; ASTM International: West Conshohocken, PA, USA, 2012.
15. ISO 14243-1:2009-11. *Implants for Surgery—Wear of Total Knee Prostheses—Part 1: Loading and Displacement Parameters for Wear-Testing Machines with Load Control and Corresponding Environmental Conditions for Test*; ISO: Geneva, Switzerland, 2009.
16. ISO 14243-3_2014-11. *Implants for Surgery—Wear of Total Knee Prostheses—Part 3: Loading and Displacement Parameters for Wear-Testing Machines with Displacement Control and Corresponding Environmental Conditions for Test*; ISO: Geneva, Switzerland, 2009.
17. ASTM F3141-17a. *Standard Guide for Total Knee Replacement Loading Profiles*; ASTM International: West Conshohocken, PA, USA, 2017.
18. Schwiesau, J.; Schilling, C.; Kaddick, C.; Utzschneider, S.; Jansson, V.; Fritz, B.; Blömer, W.; Grupp, T.M. Definition and evaluation of testing scenarios for knee wear simulation under conditions of highly demanding daily activities. *Med. Eng. Phys.* **2013**, *35*, 591–600. [CrossRef]
19. ISO 14243-5:2019-05. *Implants for Surgery—Wear of Total Knee Prostheses—Part 5: Durability Performance of the Patellofemoral Joint*; ISO: Geneva, Switzerland, 2019.
20. Halloran, J.P.; Clary, C.W.; Maletsky, L.P.; Taylor, M.; Petrella, A.J.; Rullkoetter, P.J. Verification of Predicted Knee Replacement Kinematics During Simulated Gait in the Kansas Knee Simulator. *J. Biomech. Eng.* **2010**, *132*, 081010. [CrossRef] [PubMed]
21. Ardestani, M.M.; Moazen, M.; Maniei, E.; Jin, Z. Posterior stabilized versus cruciate retaining total knee arthroplasty designs: Conformity affects the performance reliability of the design over the patient population. *Med. Eng. Phys.* **2015**, *37*, 350–360. [CrossRef]
22. Chen, Z.; Jin, Z. Prediction of in-vivo kinematics and contact track of total knee arthroplasty during walking. *Biosurf. Biotribol.* **2016**, *2*, 86–94. [CrossRef]
23. Kang, K.-T.; Koh, Y.-G.; Son, J.; Kwon, O.-R.; Baek, C.; Jung, S.H.; Park, K.K. Measuring the effect of femoral malrotation on knee joint biomechanics for total knee arthroplasty using computational simulation. *Bone Jt. Res.* **2016**, *5*, 552–559. [CrossRef] [PubMed]
24. Osano, K.; Nagamine, R.; Todo, M.; Kawasaki, M. The effect of malrotation of tibial component of total knee arthroplasty on tibial insert during high flexion using a finite element analysis. *Sci. World J.* **2014**, *2014*, 695028. [CrossRef]
25. Steinbrück, A.; Woiczinski, M.; Weber, P.; Müller, P.E.; Jansson, V.; Schröder, C. Posterior cruciate ligament balancing in total knee arthroplasty: A numerical study with a dynamic force controlled knee model. *Biomed. Eng. Online* **2014**, *13*, 91. [CrossRef]
26. Taylor, M.; Barrett, D.S. Explicit finite element simulation of eccentric loading in total knee replacement. *Clin. Orthop. Relat. Res.* **2003**, *414*, 162–171. [CrossRef]
27. Kebbach, M.; Darowski, M.; Krueger, S.; Schilling, C.; Grupp, T.M.; Bader, R.; Geier, A. Musculoskeletal Multibody Simulation Analysis on the Impact of Patellar Component Design and Positioning on Joint Dynamics after Unconstrained Total Knee Arthroplasty. *Materials* **2020**, *13*, 2365. [CrossRef] [PubMed]
28. Kang, K.-T.; Koh, Y.-G.; Son, J.; Kwon, O.-R.; Lee, J.-S.; Kwon, S.-K. Influence of Increased Posterior Tibial Slope in Total Knee Arthroplasty on Knee Joint Biomechanics: A Computational Simulation Study. *J. Arthroplast.* **2018**, *33*, 572–579. [CrossRef]
29. Woiczinski, M.; Steinbruck, A.; Weber, P.; Muller, P.E.; Jansson, V.; Schröder, C. Development and validation of a weight-bearing finite element model for total knee replacement. *Comput. Methods Biomech. Biomed. Eng.* **2016**, *19*, 1033–1045. [CrossRef]
30. Rullkoetter, P.J.; Fitzpatrick, C.K.; Clary, C.W. How Can We Use Computational Modeling to Improve Total Knee Arthroplasty? Modeling Stability and Mobility in the Implanted Knee. *J. Am. Acad. Orthop. Surg.* **2017**, *25* (Suppl. 1), S33–SS39. [CrossRef]
31. Bergmann, G.; Bender, A.; Graichen, F.; Dymke, J.; Rohlmann, A.; Trepczynski, A.; Heller, M.O.; Kutzner, I. Standardized loads acting in knee implants. *PLoS ONE* **2014**, *9*, e86035. [CrossRef]
32. Heinlein, B.; Graichen, F.; Bender, A.; Rohlmann, A.; Bergmann, G. Design, calibration and pre-clinical testing of an instrumented tibial tray. *J. Biomech.* **2007**, *40* (Suppl. 1), S4–S10. [CrossRef] [PubMed]
33. Maas, A.; Kim, T.K.; Miehlke, R.K.; Hagen, T.; Grupp, T.M. Differences in anatomy and kinematics in Asian and Caucasian TKA patients.: Influence on implant positioning and subsequent loading conditions in mobile bearing knees. *BioMed Res. Int.* **2014**, *2014*, 612838. [CrossRef]
34. Yao, J.Q.; Laurent, M.P.; Johnson, T.S.; Blanchard, C.R.; Crowninshield, R.D. The influences of lubricant and material on polymer/CoCr sliding friction. *Wear* **2003**, *255*, 780–784. [CrossRef]
35. Fricker, D.C. Friction when femoral prosthesis heads slide in acetabular cups in Ceramics in substitutive and reconstructive surgery. In Proceedings of the Satellite Symposium 3 on Ceramics in Substitutive and Reconstructive Surgery, Montecatini Terme, Italy, 27–30 June 1990; Elsevier: New York, NY, USA, 1991; pp. 207–215.
36. D'Lima, D.D.; Chen, P.C.; Colwell, C.W. Polyethylene Contact Stresses, Articular Congruity, and Knee Alignment. *Clin. Orthop. Relat. Res.* **2001**, *392*, 232–238. [CrossRef] [PubMed]
37. Ishikawa, M.; Kuriyama, S.; Ito, H.; Furu, M.; Nakamura, S.; Matsuda, S. Kinematic alignment produces near-normal knee motion but increases contact stress after total knee arthroplasty: A case study on a single implant design. *Knee* **2015**, *22*, 206–212. [CrossRef]
38. Latypova, A.; Arami, A.; Becce, F.; Jolles-Haeberli, B.; Aminian, K.; Pioletti, D.P.; Terrier, A. A patient-specific model of total knee arthroplasty to estimate patellar strain: A case study. *Clin. Biomech.* **2016**, *32*, 212–219. [CrossRef] [PubMed]
39. Wilson, W.T.; Deakin, A.H.; Payne, A.P.; Picard, F.; Wearing, S.C. Comparative analysis of the structural properties of the collateral ligaments of the human knee. *J. Orthop. Sports Phys. Ther.* **2012**, *42*, 345–351. [CrossRef]

40. Sugita, T.; Amis, A.A. Anatomic and biomechanical study of the lateral collateral and popliteofibular ligaments. *Am. J. Sports Med.* **2001**, *29*, 466–472. [CrossRef] [PubMed]

41. Trent, P.S.; Walker, P.S.; Wolf, B. Ligament Length Patterns, Strength, and Rotational Axes of the Knee Joint. *Clin. Orthop. Relat. Res.* **1976**, *117*, 263–270. [CrossRef]

42. Wijdicks, C.A.; Ewart, D.T.; Nuckley, D.J.; Johansen, S.; Engebretsen, L.; LaPrade, R.F. Structural properties of the primary medial knee ligaments. *Am. J. Sports Med.* **2010**, *38*, 1638–1646. [CrossRef] [PubMed]

43. Marinozzi, G.; Pappalardo, S.; Steindler, R. Human Knee Ligaments: Mechanical Tests and Ultrastructural Observations. *Ital. J. Orthop. Traumatol.* **1983**, *9*, 231–240.

44. Shu, L.; Yao, J.; Yamamoto, K.; Sato, T.; Sugita, N. In vivo kinematical validated knee model for preclinical testing of total knee replacement. *Comput. Biol. Med.* **2021**, *132*, 104311. [CrossRef] [PubMed]

45. Navacchia, A.; Rullkoetter, P.J.; Schütz, P.; List, R.B.; Fitzpatrick, C.K.; Shelburne, K.B. Subject-specific modeling of muscle force and knee contact in total knee arthroplasty. *J. Orthop. Res.* **2016**, *34*, 1576–1587. [CrossRef]

46. Freed, R.D.; Simon, J.C.; Knowlton, C.B.; Orozco Villaseñor, D.A.; Wimmer, M.A.; Lundberg, H.J. Are Instrumented Knee Forces Representative of a Larger Population of Cruciate-Retaining Total Knee Arthroplasties? *J. Arthroplast.* **2017**, *32*, 2268–2273. [CrossRef]

47. Kutzner, I.; Bender, A.; Dymke, J.; Duda, G.; von Roth, P.; Bergmann, G. Mediolateral force distribution at the knee joint shifts across activities and is driven by tibiofemoral alignment. *Bone Jt. J.* **2017**, *99-B*, 779–787. [CrossRef]

48. Ledingham, J.; Regan, M.; Jones, A.; Doherty, M. Radiographic patterns and associations of osteoarthritis of the knee in patients referred to hospital. *Ann. Rheum. Dis.* **1993**, *52*, 520–526. [CrossRef]

49. Fiocchi, A.; Condello, V.; Madonna, V.; Bonomo, M.; Zorzi, C. Medial vs lateral unicompartmental knee arthroplasty: Clinical results. *Acta Biomed.* **2017**, *88*, 38–44.

50. Trepczynski, A.; Kutzner, I.; Kornaropoulos, E.; Taylor, W.R.; Duda, G.N.; Bergmann, G.; Heller, M.O. Patellofemoral joint contact forces during activities with high knee flexion. *J. Orthop. Res.* **2012**, *30*, 408–415. [CrossRef] [PubMed]

51. Dahlkvist, N.J.; Mayo, P.; Seedhom, B.B. Forces during Squatting and Rising from a deep squat. *Eng. Med.* **1982**, *11*, 69–76. [CrossRef] [PubMed]

52. Reilly, D.T.; Martens, M. Experimental Analysis of the Quadriceps Muscle Force and Patello-Femoral Joint Reaction Force for Various Activities. *Acta Orthop. Scand.* **1972**, *43*, 126–137. [CrossRef]

53. Taylor, W.R.; Schütz, P.; Bergmann, G.; List, R.; Postolka, B.; Hitz, M.; Dymke, J.; Damm, P.; Duda, G.; Gerber, H.; et al. A comprehensive assessment of the musculoskeletal system: The CAMS-Knee data set. *J. Biomech.* **2017**, *65*, 32–39. [CrossRef]

54. Fox, A.J.S.; Wanivenhaus, F.; Rodeo, S.A. The basic science of the patella: Structure, composition, and function. *J. Knee Surg.* **2012**, *25*, 127–141. [CrossRef]

55. Lum, Z.C.; Saiz, A.M.; Pereira, G.C.; Meehan, J.P. Patella Baja in Total Knee Arthroplasty. *J. Am. Acad. Orthop. Surg.* **2020**, *28*, 316–323. [CrossRef] [PubMed]

5. Publication II

Title: The Influence of Mathematical Definitions on Patellar Kinematics Representations

Authors: Adrian Sauer, Maeruan Kebbach, Allan Maas, William M. Mihalko and Thomas M. Grupp

Journal: materials

Volume: 14

Issue: 24

Pages: 1–15

Year: 2021

DOI: https://doi.org/10.3390/ ma14247644

Impact factor: 3.748 (2021)

Article

The Influence of Mathematical Definitions on Patellar Kinematics Representations

Adrian Sauer [1,2,*] **, Maeruan Kebbach** [3] **, Allan Maas** [1,2] **, William M. Mihalko** [4] **and Thomas M. Grupp** [1,2]

[1] Research and Development, Aesculap AG, 78532 Tuttlingen, Germany; Allan.Maas@aesculap.de (A.M.); Thomas.Grupp@aesculap.de (T.M.G.)

[2] Department of Orthopaedic and Trauma Surgery, Musculoskeletal University Center Munich (MUM), Campus Grosshadern, Ludwig Maximilians University Munich, 81377 Munich, Germany

[3] Department of Orthopaedics, Rostock University Medical Center, 18057 Rostock, Germany; Maeruan.Kebbach@med.uni-rostock.de

[4] Campbell Clinic Department of Orthopaedic Surgery and Biomedical Engineering, University of Tennessee Health Science Center, Memphis, TN 38163, USA; wmihalko@campbellclinic.com

* Correspondence: Adrian.Sauer@aesculap.de

Abstract: A correlation between patellar kinematics and anterior knee pain is widely accepted. However, there is no consensus on how they are connected or what profile of patellar kinematics would minimize anterior knee pain. Nevertheless, answering this question by merging existing studies is further complicated by the variety of ways to describe patellar kinematics. Therefore, this study describes the most frequently used conventions for defining patellar kinematics, focusing on the rotations. The similarities and differences between the Cardan sequences and angles calculated by projecting axes are analyzed. Additionally, a tool is provided to enable the conversion of kinematic data between definitions in different studies. The choice of convention has a considerable impact on the absolute values and the clinical characteristics of the patello-femoral angles. In fact, the angles that result from using different mathematical conventions to describe a given patello-femoral rotation from our analyses differ up to a Root Mean Squared Error of $111.49°$ for patellar flexion, $55.72°$ for patellar spin and $35.39°$ for patellar tilt. To compare clinical kinematic patello-femoral results, every dataset must follow the same convention. Furthermore, researchers should be aware of the used convention's implications to ensure reproducibility when interpreting and comparing such data.

Keywords: knee joint; patello-femoral joint; kinematics; cardan sequence; euler angles; conversion

1. Introduction

Patello-femoral pain has a prevalence of more than 20% in the general population [1] and a high percentage of unsatisfied patients after total knee arthroplasty complain of anterior knee pain [2,3]. Even if satisfactory patellar tracking and kinematics seem to be evident on physical exam [4,5], it is still not entirely clear, what defines good patellar tracking and how healthy patellar kinematics can be quantified [6].

Although previous studies have investigated patellar kinematics [6,7], it remains unclear what ideal patellar kinematics encompass. What we know about patellar kinematics is that the patellar native facets or prosthetic button should be centered in the trochlear groove without subluxation or tilt throughout range of motion [6,7]. Even with descriptions of how the patella tracks from full extension to flexion, the issue of kinematic reference frame and rotations to describe motion has not been standardized.

The difficulty of converting between the multiple existing mathematical definitions of patellar kinematics or even understanding them properly is one of the major challenges for answering these questions. When we consider rotations, the way they are described has many implications. Researchers should be aware of these implications when they work with kinematic data concerning the patello-femoral joint. The choice of coordinate

systems and the mathematical definition for describing patello-femoral kinematics can lead to substantial differences in the resulting curves and how one interprets whether normal kinematics have been established. Therefore, studies without a detailed description of the underlying definitions [8–12] are of limited value for researchers and clinicians.

There is a recommendation on definitions of joint coordinate systems for various joints from the International Society of Biomechanics. However, they do not provide a recommended definition for the knee joint, especially not for the patello-femoral joint [13–15]. However, since the publication of these recommendations, a lot of research has been conducted for the patello-femoral joint kinematics. To describe these kinematics, a definition using a floating axis for patellar spin [16], which has been recommended by Bull et al. [17], has been increasingly used in the past few years. This definition follows the same principle used by Grood and Suntay [18] for the tibio-femoral joint.

Nevertheless, there are still lots of studies that use more uncommon conventions for patello-femoral rotations which can lead to fundamental changes in the values for patellar flexion, spin and tilt [6,17]. Therefore, for interpretation of patello-femoral kinematics data a clear understanding of the underlying conventions is needed. If data with different underlying definitions should be compared, the ability to transform between several conventions is very helpful, but rarely described in literature.

The aim of this article is to give an overview of the different methods that can be used to describe patellar kinematics, with a particular focus on rotations. In contrast to previous publications, this article will consider the implications associated with each definition in greater detail. Additionally, the mathematics behind the patellar rotations will be given, including ways to convert data between some of the most common definitions. Therefore, the purpose is to enable researchers to choose the definition of patellar kinematics that is most suitable to them, as well as allow them to easily perform any conversions necessary to be able to compare the outcomes of different studies. As Supplementary Material, a Matlab template is provided to perform the most common conversions easily.

2. Materials and Methods

2.1. Coordinates and Definitions

In the following description, two reference frames will mainly be used: one attached to the femur and another to the patella, with the directions x, y and z pointing laterally, anteriorly and proximally, respectively, in full extension. If the femur or patella rotate and translate during flexion, the attached coordinate systems will follow the bones' movements. Figure 1 shows a possible system of axes for the patellar kinematics. Since the exact orientation depends on the chosen definition, it is neither described nor shown in more detail. The question of how these directions can be identified, i.e., which landmarks can be used, is highly dependent on the data and the measurement methods of every single study and will therefore not be deeply discussed. A possibility to define a reference frame for the patella is presented and validated by Innocenti et al. [19].

The most clinically relevant kinematic parameters are patellar shift, patellar flexion (α), spin (β) and tilt (γ) [5,17,20–22]. The patella's resulting movements are relative to the femur as follows: patellar flexion is defined by the relative rotation of the patella around the medio-lateral flexion axis (*x*-axis). In most cases, the *femoral* flexion axis is used as the rotation axis for patellar flexion. In a clinical context, patellar spin and tilt are represented by the rotations around the local *patellar* y- and z-axes, respectively. Alternatively, it is also common to use a floating axis for patellar tilt [23,24] or patellar spin [25–27]. The patellar shift is the translation of the patella in the medio-lateral direction with respect to the femur or the trochlear groove. Usually, the patellar shift is given as the patellar movement in the direction of the *femoral x*-axis, which can be calculated by projecting the vector of the relative patellar translations on the normalized direction of the femoral flexion axis. The values of shift, flexion, spin and tilt for a given instance of patellar motion can differ considerably from this intuitive understanding if different definitions are used.

Figure 1 shows the described components of the patellar kinematics schematically without giving precise axes and signs because these are dependent on the chosen definition.
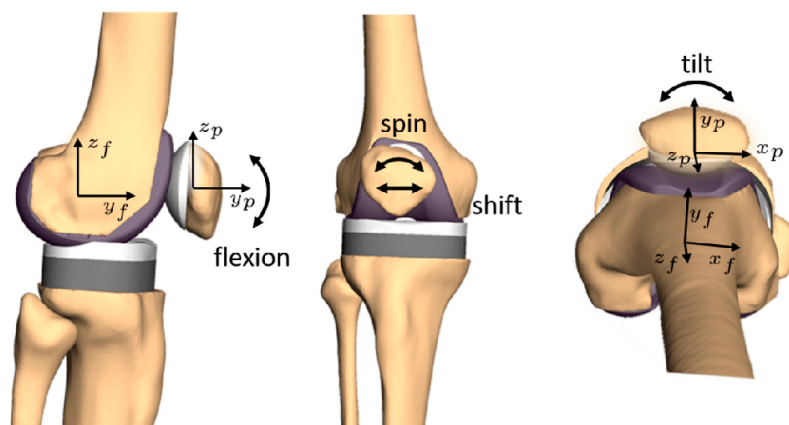

Figure 1. Overview on patellar kinematics and underlying coordinate systems. (**Left**): patellar flexion in a sagittal view, (**center**): medio-lateral movement (shift) and patellar spin in an anterior view, (**right**): patellar tilt in a proximal view. The exact location and orientation of the rotation axes depend on the chosen definition and is therefore not shown in detail. The patellar axes are labelled with x_p, y_p, z_p and the femoral axes with x_f, y_f, z_f.

The movements of the patella in the sagittal plane are highly dependent on the definition of the origin of the femoral coordinate system. If individual anatomical landmarks are used to define this origin, the comparison between different subjects can be problematic. However, since these movements are of secondary clinical interest [17] and are controlled mainly by joint geometry [28], they are not discussed here.

2.2. How Rotations Can Be Described

There are several ways to describe the rotational state of an object in a coordinate system. For example, well-known methods include rotational matrices, quaternions, projected angles, helical axes, and extrinsic and intrinsic rotation sequences. In biomechanics, representations allowing the comparison of rotations around the individual joint axes are needed. Therefore, rotation matrices, quaternions and helical axes are only suitable to process data, but not to interpret the results of studies according to patellar kinematics.

First, a fundamental property of rotations should be noted: rotations are not commutative. This means that—regardless of the mathematical description—the resulting pose for a sequence of rotations about multiple axes is generally not equal to the same rotations in another sequence. This statement remains valid for both multiple rotations in time and rotation sequences to describe a pose at one point in time.

To describe any rotation in three-dimensional (3D) space, a rotation sequence consisting of three consecutive rotations around three axes can be used. If the orientation of the axes is changed by each elemental rotation, the sequence is referred to as *intrinsic*. For initial coordinate axes ξ, η, ζ, the axes after the first rotation are written as ξ', η', ζ' and after the second rotation as ξ'', η'', ζ''. If all rotations occur around the axes as they are in their initial orientation, independent of previous rotation steps, the rotation sequence is called an *extrinsic* rotation.

In biomechanical literature, sometimes an intrinsic sequence of rotations around *three different axes* is called an Euler rotation, and the associated angles are termed *Euler angles* [29,30]. The correct term for these angles is in fact *Cardan angles* or *Tait-Bryan-angles*. Actual Euler angles are an intrinsic rotation sequence, which uses the same axis for the first and the third rotation (e.g., rotations around the axes ξ, η', ξ'') [31]. While Cardan angles

can be used for a biomechanical description of patello-femoral rotations, Euler angles are difficult to relate to the clinical terms of patellar flexion, spin and tilt. Figure 2 shows three different rotation sequences which lead to a particular patellar orientation.
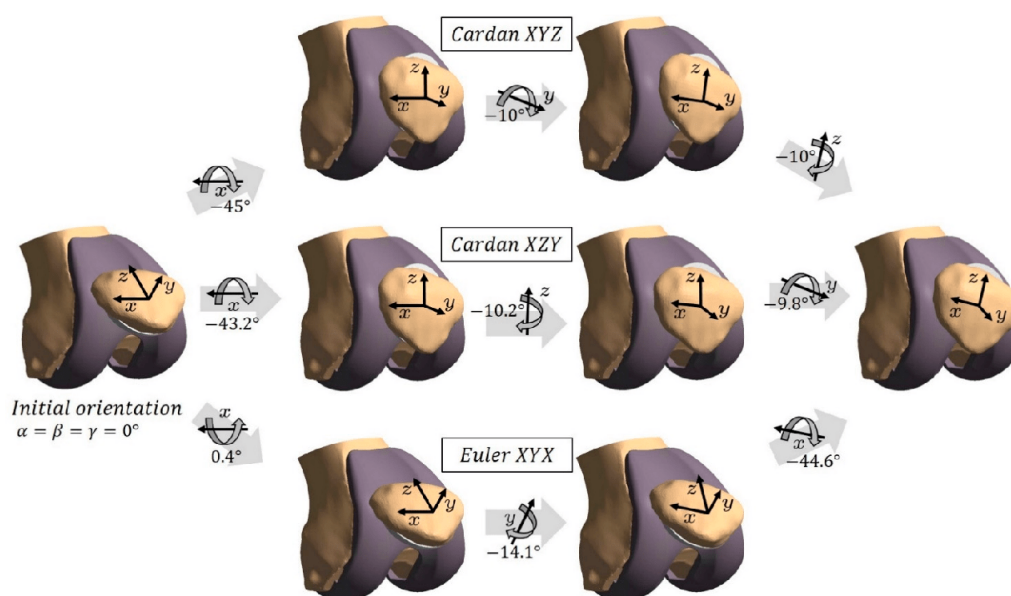

Figure 2. Illustration of three exemplary rotation sequences representing one particular patellar orientation. All sequences start in a patellar orientation where the patellar axes are parallel to the femoral axes. The upper and middle paths show the Cardan sequences XYZ and XZY, respectively, and the lower path represents the Euler sequence XYX.

Two disadvantages are occasionally associated in connection with Cardan angles. The first, sequence dependency, can simply be solved by appropriate standardization of the sequence [32]. The second is termed gimbal lock, which occurs when the second angle of the sequence is $\pm 90°$ [33]. In this case, the axes of the first and third rotation are collinear, and one degree of freedom is lost. Since the patellar spin and tilt do not reach absolute values of $90°$ [6,7] sequences with either of these in the middle position are free from this problem for the description of patellar kinematics.

If femoral axes are used to describe the patello-femoral rotations [34], the interpretation of the rotations around the femoral anterior-posterior and proximo-distal axes as patellar spin and patellar tilt, respectively, are in general no longer correct. For a patellar flexion near $0°$ the deviation remains small, but for one of $90°$ the femoral tilt axis is parallel to the patellar spin axis in a sagittal view. The same applies to the femoral rotation axis and the patellar tilt axis. In this case, the calculated values for tilt and spin of the patella are switched, in addition to a possible inversion of their sign, relative to the common clinical interpretation [17] (see also Figure 3). Researchers should be aware that Cardan sequences ending with patellar flexion (ZYX and YZX) show the same pattern (e.g., [35]).

For knee kinematics, it seems that there exists another valuable way to describe the rotations. It is called the *three-cylinder open-chain representation*. For the tibio-femoral joint, it was first mentioned by Grood and Suntay in 1983 [18]. It was suggested in 2009 by Merican and Amis [36] and later on proven in 2014 by MacWilliams and Davis [37] that the Grood and Suntay definition is equivalent to a Cardan XYZ-sequence. This sequence was regardless found suitable to describe the tibio-femoral kinematics [38,39].
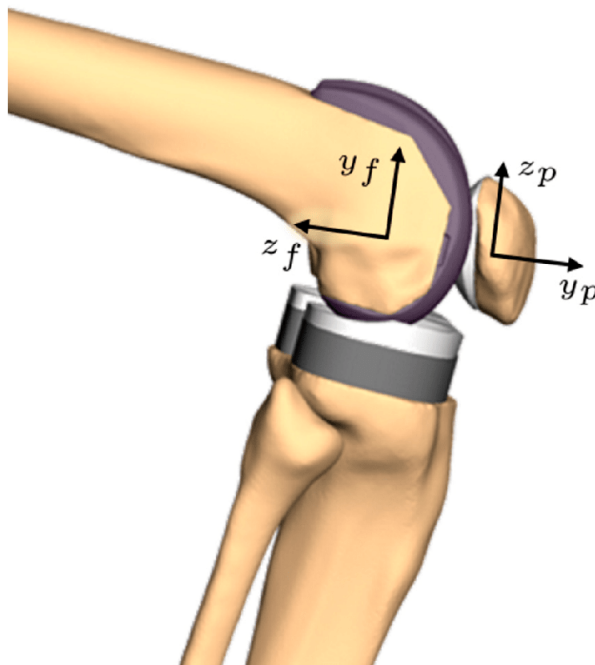
Figure 3. Illustration of the switch of meaning of patellar spin and tilt for an absolute patellar flexion angle of 90°, if described with respect to the femoral coordinate system. Rotating the patella around the anatomical patellar proximo-distal axis (z_p) equals a rotation around the femoral anterior-posterior axis (y_f) for 90° of patello-femoral flexion. The z_f- and y_p-axes show a similar pattern.

For the patello-femoral joint, the three-cylinder open-chain representation was first applied in 1992 by Hefzy et al. [16]. Since this way to describe patellar kinematics was recommended in a method paper [17], it is frequently used. The proof of the equivalence of the Grood and Suntay rotations and a Cardan sequence for the tibio-femoral joint [37] can be carried out analogously for the patello-femoral joint. Therefore, the three-cylinder open-chain representation of the patello-femoral kinematics is—from the rotations point of view—equivalent to the use of the Cardan sequence XYZ. Since Bull et al. [17] do not describe translations in a sagittal plane, their recommendation is to measure the patellar shift relative to the femoral medio-lateral axis and describe the patellar rotations with respect to the femoral axes as a Cardan XYZ-sequence.

The methods, which use a sequence of rotations around rotated or not rotated co-ordinate axes, lead to the inherent possibility to receive a description of the pose of the associated body very straightforward by executing the rotations one after the other. Nevertheless, some authors [40,41] determine the rotations of the patella by projecting the patellar coordinate vectors on the planes of the femoral coordinate system and calculate the angle between these projected vectors and the associated vectors from the femoral system. For instance, the patellar flexion can be calculated by projecting the y-vector of the patella onto the sagittal plane of the femoral coordinate system and calculating the angle between this projection and the y-vector of the femoral system. If a projection is carried out onto the patellar coordinate planes, a rotation relative to the patellar axes can be calculated. This method in general does not lead to values for patellar flexion, spin and tilt which can be executed in sequence to acquire the full rotation of the patella relative to the femur. For every projection plane, there are two vectors that can be projected to calculate the rotation around the axis perpendicular to this plane. As the results of this paper will show, the calculated angles for these two projected directions differ a lot for

3D rotations. For example, the calculation of the patellar flexion as the angle between the patellar *y*-axis projected onto the sagittal plane of the femoral system differs from the same calculation with the z-axes. Therefore, the angles are highly dependent on the choice of planes and axes.

2.3. Conversions

A method to convert a rotation from one definition to another is to calculate the rotation matrix representing the rotation and use this matrix to calculate the parameters of the desired definition. To that end, methods will be given to convert the common definitions into matrix form and back. Figure 4 shows an overview of the conversion paths introduced in this paper. The conversions are first given for intrinsic and extrinsic rotation sequences.
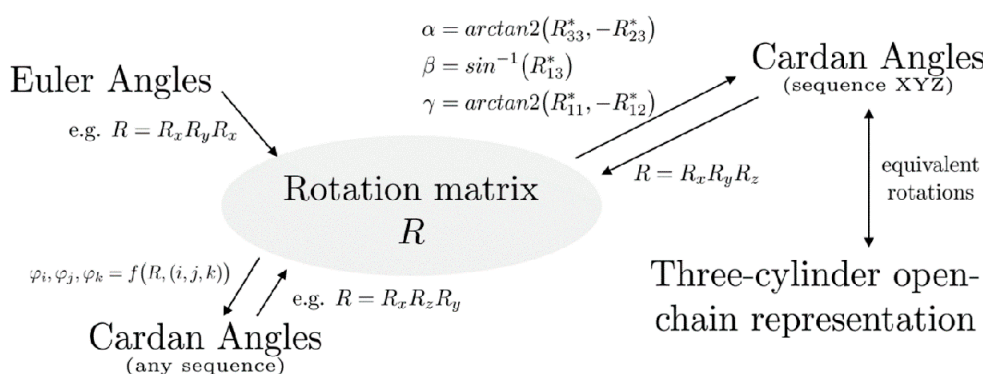

Figure 4. Overview of transformation paths between different descriptions of patellar rotations.

2.3.1. Rotation Sequences

With the standard uniaxial 3D rotation matrices $R_x(\alpha)$, $R_y(\beta)$ and $R_z(\gamma)$ for the rotations around x, y and z, the rotation matrix R of the full 3D rotation can be calculated by matrix multiplication. For an extrinsic rotation sequence, the resulting matrix R is the matrix product of the corresponding uniaxial rotation matrices, expressed in the opposite sequence order from left to right. For an intrinsic rotation sequence, the order of the uniaxial rotation matrices is inverted. For example, the rotation matrix $R = R_x(\alpha) \cdot R_y(\beta) \cdot R_z(\gamma)$ represents the extrinsic rotation sequence ZYX and the intrinsic sequence XYZ. It is important to note that this method works the same for Euler angles.

The formulas for calculating the angles α, β and γ for a specific sequence from a given rotation matrix R* with the entry R_{st}* in line *s* and column *t* are obviously dependent on the sequence. Rotating around a particular axis twice within one sequence leads to angles that are hard to interpret clinically. Only the equations for Cardan angles are therefore given here.

For certain sequences, the following method is often shown in literature (e.g., intrinsic XYZ-sequence [32,42]). Here, a general formulation which can be used for any sequence, will be introduced.

Let (i,j,k) be a tuple of three different indices with (i,j,k) ∈ {1,2,3}. Then every (i,j,k)-tuple represents a Cardan sequence (e.g., (i,j,k) = (1,3,2) stands for the sequence XZY). To calculate the angles of the patello-femoral rotations, the sign sgn_{ijk} of a sequence tuple is needed. The sign is equal to 1 if the tuple (i,j,k) can be created from the tuple (1,2,3) by an even number of transpositions. If the number of transpositions is odd, sgn_{ijk} is equal to −1 [43]. The equations

$$\varphi_i = \text{arctan2} \left(R_{kk}^*, -sgn_{ijk} \cdot R_{jk}^*\right) \tag{1}$$

$$\varphi_j = \sin^{-1} \left(sgn_{ijk} \cdot R_{ik}^*\right) \text{ and} \tag{2}$$

$$\varphi_k = \arctan 2\ (R_{ii}{}^*,\ -\mathrm{sgn}_{ijk} \cdot R_{ij}{}^*) \tag{3}$$

directly lead to the sought angles for flexion ($\alpha = \varphi 1$), spin ($\beta = \varphi_2$) and tilt ($\gamma = \varphi_3$). The proof for Equations (1)–(3) is given in the Supplementary Materials.

2.3.2. Projected Angles

For the reconstruction of the 3D orientation from projected angles, giving a closed description of all 64 possible axis-plane projection combinations is not feasible in this article. Only a brief overview of the derivation of the equations will be given here. Every given projected angle can be used to determine a semicircle containing all the unit vectors that would lead to this angle if projected. If the j-th axis is projected onto the femoral (or patellar) coordinate plane, the parametrized semicircle can be set to equal the j-th column (or row, in the case of the patellar plane) vector of the rotation matrix. The orthogonality of rotation matrices (pairwise orthogonality of rows and columns, Euclidian norm of every row and column equals 1, third row/column is cross product of first and second row/column) gives the conditions to determine the parameters and the missing entries of R.

2.3.3. Helical Axes

Helical axes are a way to represent a 3D-movement using only one rotation axis for every time step. The movement is described as a translation along this axis and a rotation around it. This method is sometimes used to analyze the actual joint rotation axis, especially for the tibio-femoral joint [44,45]. This description has also been sometimes used for the patello-femoral joint [46,47]. Consequently, the ideas for the conversion of the rotations are discussed here briefly.

The direction of the rotation axis is given by the helical axis. Thus, the Rodrigues' rotation formula [48] can be used to rotate a vector around any given rotation axis. Matrix representation of a helical axis rotation can be achieved by applying this formula to the unit vectors. The rotated unit vectors give the columns of the associated rotation matrix. For the opposite conversion, the direction of this axis is the eigenvector to the eigenvalue of 1, while the angle can be obtained from the other eigenvalues [49,50]. For more details [51] is recommended.

2.3.4. Three-Cylinder Open-Chain Representation

As stated previously, the angles in the three-cylinder open-chain representation [16,17] are equivalent to the angles of the intrinsic XYZ rotation sequence. Therefore, the methods used for this sequence can also be applied to convert rotations from or into this convention.

2.4. Data Processing and Validation

To compare the definitions described earlier in this paper, kinematic data from a previously published and validated musculoskeletal model of the lower right extremity simulating a squat motion [20] was used. This simulation model was implemented in the software SIMPACK (V9.7, Dassault Systèmes Deutschland GmbH, Gilching, Germany). The rotations of the patella relative to the femur were evaluated for a squat motion in all possible Cardan sequences directly in the software. These were used as reference data for verifying the implementation of the previous formulas in MATLAB (R2018a, Mathworks, Natick, Massachusetts, USA). The deviations between the curves were quantified by calculating the Root Mean Squared Error (RMSE).

3. Results

The dataset for a squat includes tibio-femoral flexion angles from $0°$ to $90°$. The discrepancy between the angles according to the different definitions increases with the tibio-femoral flexion angles. Based on the data for the Cardan XYZ-sequence, the angles for the five remaining Cardan sequences and the projected angles were calculated. In order to validate the conversion process, the Cardan sequences for the same dataset were evaluated directly from the general multibody software SIMPACK as reference. The

deviation of these results to the values from converting the XYZ data do not exceed $0.0001°$ (RMSE $< (6.13 \times 10^{-5})°$ for all sequences and angles).

3.1. Cardan Angles

Figure 5 shows the rotation angles for all possible Cardan sequences. The choice of definition has a minor effect on the patellar flexion values. All Cardan sequences except for ZXY have very similar flexion angles. The maximum RMSE within this group is $0.79°$ (see also Table 1). The patellar flexion angle of the ZXY-sequence differs up to $7.83°$ from the others (RMSE $\geq 3.71°$).
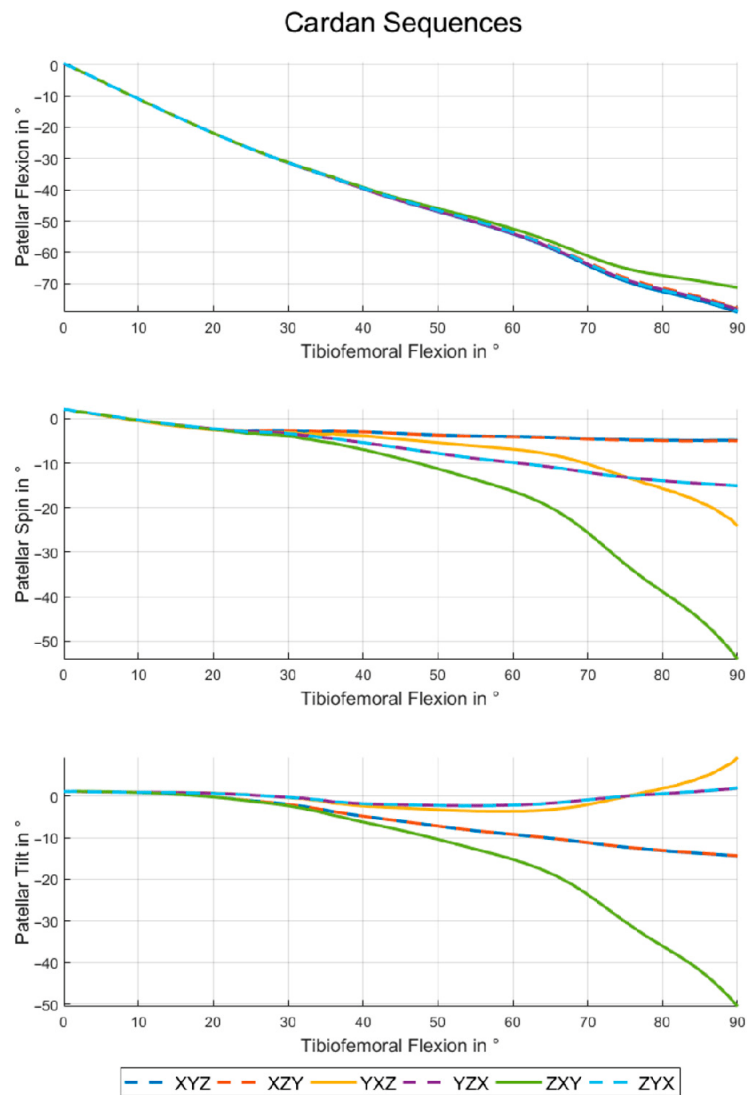

Figure 5. Patellar kinematics for the Cardan sequences. Patellar flexion (**top**), spin (**center**) and tilt (**below**) during a squat motion for all Cardan sequences.

Table 1. RMSE of patellar flexion curves for Cardan sequences and projected angles in °.

	XYZ	XZY	YXZ	YZX	ZXY	ZYX	Y on Patella	Z on Patella	Y on Femur	Z on Femur
XYZ	0	-	-	-	-	-	-	-	-	-
XZY	0.79	0	-	-	-	-	-	-	-	-
YXZ	0.46	0.36	0	-	-	-	-	-	-	-
YZX	0.43	0.4	0.05	0	-	-	-	-	-	-
ZXY	3.71	2.96	3.25	3.28	0	-	-	-	-	-
ZYX	0.39	0.44	0.26	0.25	3.4	0	-	-	-	-
Y on patella	111.48	110.71	111.06	111.09	108.11	111.1	0	-	-	-
Z on patella	111.49	110.72	111.07	111.1	108.12	111.12	0.25	0	-	-
Y on femur	0.79	0	0.36	0.4	2.96	0.44	110.71	110.72	0	-
Z on femur	0	0.79	0.46	0.43	3.71	0.39	111.48	111.49	0.79	0

In terms of patellar spin and patellar tilt the Cardan XYZ- and XZY-sequences are very close (spin: RMSE = 0.09° and tilt: RMSE = 0.03°) as Tables 2 and 3 show. The same is true for YZX and ZYX (spin: RMSE = 0.004° and tilt: RMSE = 0.03°). The sequence ZXY leads to curves which differ considerably from those of other sequences (RMSE up to 27.72°). These deviations are particularly large and grow increasingly for higher tibio-femoral flexion angles, and reach a maximum of 49.22° for the patellar spin and 59.91° for the patellar tilt.

Table 2. RMSE of patellar spin curves for Cardan sequences and projected angles in °.

	XYZ	XZY	YXZ	YZX	ZXY	ZYX	X on Patella	Z on Patella	X on Femur	Z on Femur
XYZ	0	-	-	-	-	-	-	-	-	-
XZY	0.09	0	-	-	-	-	-	-	-	-
YXZ	8.27	8.18	0	-	-	-	-	-	-	-
YZX	6.56	6.48	3.09	0	-	-	-	-	-	-
ZXY	24.37	24.28	16.19	18.06	0	-	-	-	-	-
ZYX	6.56	6.48	3.09	0.004	18.06	0	-	-	-	-
X on patella	7.85	7.93	15.47	14.24	31.53	14.24	0	-	-	-
Z on patella	31.44	31.53	39.56	37.94	55.72	37.94	24.28	0	-	-
X on femur	6.56	6.48	3.09	0	18.06	0.004	14.24	37.94	0	-
Z on femur	8.27	8.18	0	3.09	16.19	3.09	15.47	39.56	3.09	0

Table 3. RMSE of patellar tilt curves for Cardan sequences and projected angles in °.

	XYZ	XZY	YXZ	YZX	ZXY	ZYX	X on Patella	Y on Patella	X on Femur	Y on Femur
XYZ	0	-	-	-	-	-	-	-	-	-
XZY	0.03	0	-	-	-	-	-	-	-	-
YXZ	11.07	11.04	0	-	-	-	-	-	-	-
YZX	9.64	9.61	2.27	0	-	-	-	-	-	-
ZXY	16.69	16.72	27.72	26.14	0	-	-	-	-	-
ZYX	9.65	9.62	2.24	0.03	26.15	0	-	-	-	-
X on patella	19.36	19.33	9.38	9.92	35.39	9.91	0	-	-	-
Y on patella	9.38	9.35	6.79	4.67	24.45	4.7	11.07	0	-	-
X on femur	9.65	9.62	2.24	0.03	26.15	0	9.91	4.7	0	-
Y on femur	16.69	16.72	27.72	26.14	0	26.15	35.39	24.45	26.15	0

3.2. Projected Angles

The projected angles can be divided into two groups. Projecting the patellar reference frame vectors onto the femoral planes gives patello-femoral rotations with respect to the femoral system. Therefore, the angles for patellar flexion are close to the negative of the

angles obtained by projecting onto the patellar planes (see also Figure 6, top). The flexion angles calculated by projecting the *y*- (or *z*-) axis on the femoral standard plane are equal to the patellar flexion angles from the Cardan XZY- (or XYZ- for the *z*-axis) sequence as the RMSE of 0° for these combinations shows in Table 1. The same pattern is visible for the patellar spin and tilt if the projections on femoral planes and Cardan sequences starting with y- and z-axes are analyzed (see also Tables 2 and 3).
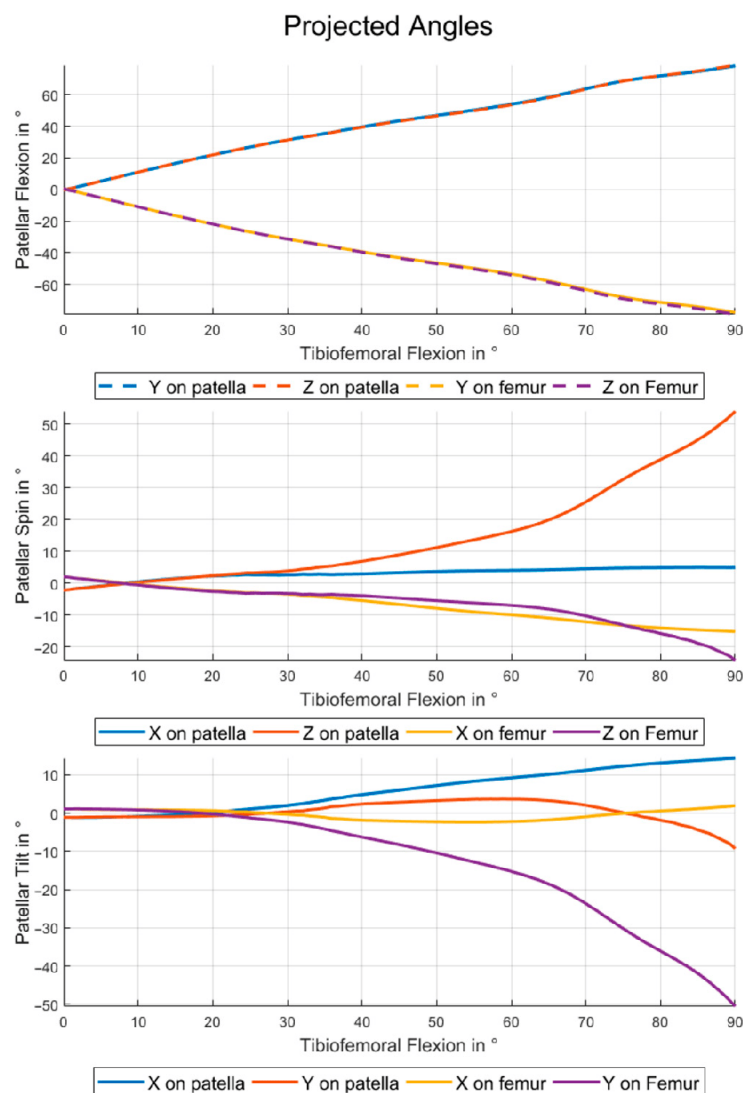
Figure 6. Patellar kinematics using projected angles. Patellar flexion (**top**), spin (**center**) and tilt (**below**) during a squat motion for all possible ways to calculate the angles by projection.

4. Discussion

The first objective of this study was to show the considerable impact of different mathematical definitions on how patello-femoral kinematics are conveyed. A framework was thereby developed to enable researchers to choose the definitions for the patellar kinematics which best fit their needs and to convert patellar kinematics between the

different conventions. In this way, comparability and interchangeability between different studies may be facilitated.

The results obtained from the conversions we have presented using the described formulas are in excellent agreement with those obtained from the evaluation using a general multibody software package (RMSE $< (6.13 \times 10^{-5})°$ for all sequences and angles). Therefore, the derived equations and their implementation were verified.

The presented results indicate clearly that the chosen definition for patello-femoral angles has an impact on the description of patello-femoral kinematics. The curves for patellar flexion, spin and tilt deviate not only in magnitude but also in their characteristics (see Figures 5 and 6). Therefore a correct interpretation of patello-femoral kinematic data seems to be impossible if the details of the convention used are not clear.

Deviations between the results with different definitions only occur if rotations around at least two standard directions differ from zero. This condition is based on the fact that the differences are caused by changes in rotation axes for subsequent rotations. For increasing tibio-femoral flexion angles the absolute patellar flexion angle reaches values close to 80°, while the absolute values of patellar spin and tilt stay relatively small if the rotations are considered around the patellar axes. Therefore, the rotation around the *x*-axis and its position in the Cardan sequence has a special impact on the data for high tibio-femoral and patello-femoral flexion angles. In the case of small patellar spin and tilt, it can be assumed that the rotation axes that occur before the patellar flexion in the Cardan sequence almost agree with the associated femoral coordinate system axes. The rotations placed after the flexion in the sequence can be interpreted as rotations around associated patellar body axes. For the first and last rotations of a Cardan sequence these statements are exactly true.

For the patello-femoral kinematics this means that the first rotation of a sequence is always around the associated axis of the femoral coordinate system and the last rotation is around a patella-fixed axis, as previously shown in Figure 2. The floating axis between these two is close to the associated patellar axis if the sequence starts with the patellar flexion and is close to the associated femoral axis otherwise. In accordance with the previous explanations the two Cardan sequences starting and ending with the patellar flexion (XYZ/XZY and YZX/ZYX) show very small differences (see Figure 5, and Tables 1–3).

For 90° of absolute patellar flexion angle patellar spin and tilt would swap its values if the patellar flexion would be changed from the first position (i.e., tilt and spin close to patellar body fixed rotations) to the third position (i.e., tilt and spin close to femoral body fixed rotation). This is caused by the inherent change from patellar to femoral coordinate system. For the squat cycle showed here, only 80° of absolute patellar flexion are reached. Nevertheless, the described effect can be seen, if the maximum patellar tilt for the sequences XYZ and XZY (15.0°) is compared to the patellar spin for YZX and ZYX (15.7°).

One of the main difficulties in using Cardan sequences to describe rotational poses is the gimbal lock, which occurs if the second rotation of the sequence is equal to 90°. In this case, the axis of the third rotation is parallel to the direction of the first one (or its negative) and the rotation loses one degree of freedom. The absolute values for spin and tilt are far from 90° for healthy knees [6,7]. Therefore, this situation only exists if the patellar flexion is the second rotation of the sequence. Even if the maximum absolute values for patellar flexion in the shown results are less than 80°, an increase of spin and tilt can be mentioned for the YXZ sequence and a comparably larger one for the ZXY sequence. (see Tables 2 and 3). The reason why ZXY differs more from the sequences without the x-rotation on second position than YXZ is that the patello-femoral rotation around the femoral *z*-axis is bigger than around the femoral *y*-axis. These effects are making the interpretation of the patellar kinematics in the ZXY and YXZ sequence quite laborious and this description differs a lot from a clinical understanding for spin and tilt. Therefore these sequences are not recommended.

The projected angles also show big differences dependent on the choice of which axis is projected onto which coordinate system. Figure 6 indicates clearly that this method is very sensitive to the choice of projection axis and that this effect increases with growing

angles in the other two dimensions. The flexion angles are robust against switching from *y*- to *z*-axis for projection, while comparable changes for spin and tilt cause completely different curves due to the relatively higher patellar flexion angles.

For small angles of spin and tilt the projected angles for flexion on the patellar (or femoral) planes can be interpreted as flexion with respect to the patellar (or femoral) system. Due to the high flexion angles, the same interpretation cannot be applied to spin and tilt. For spin and tilt the values are also highly depending on the choice of axis for projection.

It was shown that the deviations between the curves for patellar flexion, spin and tilt for the different kinematic definitions can completely change in both, magnitude and characteristics of the curves. Nevertheless, the differences are not big enough in every case that inadvertently comparing results based on different definitions would be obvious at first glance. Therefore the problem explored by this study should always be considered when dealing with patellar kinematics.

Patellar maltracking is known as possible cause of anterior knee pain [4,5,52–55], but it still remains unknown, how critical patellar kinematics can be distinguished from others [6]. To increase the biomechanical knowledge about how anterior knee pain can be prevented or treated, it will help to bring the available data from the literature together. Therefore, it is essential to properly understand the underlying definitions of every single study and to carefully transform the data into one representation, that can be compared across the available literature. For most of the studies available in literature the given transformations from this study can be utilized.

If researchers are free to choose a convention for their own study, the use of Cardan sequences is recommended due to the available straight forward methods for calculation, conversion and interpretation. Even if all Cardan sequences are theoretically suitable to represent the patello-femoral kinematics in a correct way, some of them are better for intuitive interpretation from a biomechanical side of view. The definitions which are closest to the clinical understanding of patellar flexion, tilt and spin are the two Cardan sequences beginning with patellar flexion (XYZ and XZY), where patellar flexion is given around the *femoral* flexion axis. The last rotation of the sequence is given exactly around the associated *patellar* axis while the second rotation of the sequence is executed around the floating axis perpendicular to the other two. Therefore, the rotation (out of spin and tilt) with the most importance for a certain study should be chosen as last rotation of the sequence. The higher clinical relevance of tilt compared to patellar spin will qualify the Cardan sequence XYZ as recommendation for most studies.

5. Conclusions

In this study the most common definitions for patello-femoral rotations and the most important conversions between them were described. Using kinematic data of a validated squat motion based on motion capture, it was shown that the angles describing the patellar kinematics are highly dependent on the underlying convention.

If researchers are not aware of the described deviations, misinterpretation of results is very likely, which is critical for clinically relevant studies. Additionally, the comparison of different studies should only be executed if equivalence of the used conventions can be ensured or if the data are carefully transformed. Therefore, the methods from this study will help to uncover the complex relationship between patellar kinematics and anterior knee pain.

Author Contributions: Conceptualization, A.S., M.K., A.M., W.M.M. and T.M.G.; methodology, A.S. and M.K.; software, A.S.; validation, A.S. and M.K.; formal analysis, A.S.; investigation, A.S. and M.K.; resources, A.S., M.K., A.M. and T.M.G.; data curation, A.S. and M.K.; writing—original draft

preparation, A.S.; writing—review and editing, A.S., M.K., A.M., W.M.M. and T.M.G.; visualization, A.S. and M.K.; supervision, A.M. and T.M.G.; project administration, A.S., A.M. and T.M.G.; funding acquisition, A.M. and T.M.G. All authors have read and agreed to the published version of the manuscript.

Funding: Three of the authors (A.S., A.M., T.M.G.) were funded by B.Braun Aesculap AG, Tuttlingen, Germany. The funder provided support in the form of salaries for authors A.S., A.M. and T.M.G. The funders had no role in study design, data collection and analysis, decision to publish, or preparation of the manuscript.

Institutional Review Board Statement: Not applicable.

Informed Consent Statement: Not applicable.

Data Availability Statement: The dataset used for this study is available as Supplementary Material (S3).

Conflicts of Interest: Three of the authors (A.S., A.M., T.M.G.) are employees of B.Braun Aesculap AG, Tuttlingen, Germany. W.M.M. is a paid consultant at B. Braun Aesculap AG, but did not receive any reimbursement for the current study. M.K. declares no conflicts of interest.

References

1. Smith, B.E.; Selfe, J.; Thacker, D.; Hendrick, P.; Bateman, M.; Moffatt, F.; Rathleff, M.S.; Smith, T.O.; Logan, P. Incidence and prevalence of patellofemoral pain: A systematic review and meta-analysis. *PLoS ONE* **2018**, *13*, e0190892. [CrossRef]
2. Parvizi, J.; Rapuri, V.R.; Saleh, K.J.; Kuskowski, M.A.; Sharkey, P.F.; Mont, M.A. Failure to resurface the patella during total knee arthroplasty may result in more knee pain and secondary surgery. *Clin. Orthop. Relat. Res.* **2005**, *438*, 191–196. [CrossRef]
3. Steinbruck, A.; Schröder, C.; Woiczinski, M.; Muller, T.; Muller, P.E.; Jansson, V.; Fottner, A. Influence of tibial rotation in total knee arthroplasty on knee kinematics and retropatellar pressure: An in vitro study. *Knee Surg. Sports Traumatol. Arthrosc.* **2016**, *24*, 2395–2401. [CrossRef]
4. Powers, C.M.; Witvrouw, E.; Davis, I.S.; Crossley, K.M. Evidence-based framework for a pathomechanical model of patellofemoral pain: 2017 patellofemoral pain consensus statement from the 4th International Patellofemoral Pain Research Retreat, Manchester, UK: Part 3. *Br. J. Sports Med.* **2017**, *51*, 1713–1723. [CrossRef] [PubMed]
5. Wheatley, M.G.A.; Rainbow, M.J.; Clouthier, A.L. Patellofemoral Mechanics: A Review of Pathomechanics and Research Approaches. *Curr. Rev. Musculoskelet. Med.* **2020**, *13*, 326–337. [CrossRef] [PubMed]
6. Yu, Z.; Yao, J.; Wang, X.; Xin, X.; Zhang, K.; Cai, H.; Fan, Y.; Yang, B. Research Methods and Progress of Patellofemoral Joint Kinematics: A Review. *J. Healthc. Eng.* **2019**, *2019*, 9159267. [CrossRef]
7. Katchburian, M.V.; Bull, A.M.J.; Shih, Y.-F.; Heatley, F.W.; Amis, A.A. Measurement of patellar tracking: Assessment and analysis of the literature. *Clin. Orthop. Relat. Res.* **2003**, *412*, 241–259. [CrossRef] [PubMed]
8. Chew, J.T.; Stewart, N.J.; Hanssen, A.D.; Luo, Z.-P.; Rand, J.A.; An, K.-N. Differences in Patellar Tracking and Knee Kinematics Among Three Different Total Knee Designs. *Clin. Orthop. Relat. Res.* **1997**, *345*, 87–98. [CrossRef]
9. Nakamura, S.; Tanaka, Y.; Kuriyama, S.; Nishitani, K.; Ito, H.; Furu, M.; Matsuda, S. Superior-inferior position of patellar component affects patellofemoral kinematics and contact forces in computer simulation. *Clin. Biomech.* **2017**, *45*, 19–24. [CrossRef]
10. Sakai, N.; Luo, Z.-P.; Rand, J.A.; An, K.-N. The effects of tibial rotation on patellar position. *Knee* **1994**, *1*, 133–138. [CrossRef]
11. Sakai, N.; Luo, Z.-P.; Rand, J.A.; An, K.-N. Quadriceps forces and patellar motion in the anatomical model of the patellofemoral joint. *Knee* **1996**, *3*, 1–7. [CrossRef]
12. Sakai, N.; Luo, Z.-P.; Rand, J.A.; An, K.-N. The influence of weakness in the vastus medialis oblique muscle on the patellofemoral joint: An in vitro biomechanical study. *Clin. Biomech.* **2000**, *15*, 335–339. [CrossRef]
13. Wu, G.; Cavanagh, P.R. ISB recommendations for standardization in the reporting of kinematic data. *J. Biomech.* **1995**, *28*, 1257–1261. [CrossRef]
14. Wu, G.; Siegler, S.; Allard, P.; Kirtley, C.; Leardini, A.; Rosenbaum, D.; Whittle, M.; D'Lima, D.D.; Christofolini, L.; Witte, H.; et al. ISB recommendation on definitions of joint coordinate system of various joints for the reporting of human joint motion: Part I: Ankle, hip, and spine. *J. Biomech.* **2002**, *35*, 543–548. [CrossRef]
15. Wu, G.; van der Helm, F.C.T.; Veeger, H.E.J.D.; Makhsous, M.; van Roy, P.; Anglin, C.; Nagels, J.; Karduna, A.R.; McQuade, K.; Wang, X.; et al. ISB recommendation on definitions of joint coordinate systems of various joints for the reporting of human joint motion–Part II: Shoulder, elbow, wrist and hand. *J. Biomech.* **2005**, *38*, 981–992. [CrossRef]
16. Hefzy, M.S.; Jackson, W.T.; Saddemi, S.R.; Hsieh, Y.-F. Effects of tibial rotations on patellar tracking and patello-femoral contact areas. *J. Biomed. Eng.* **1992**, *14*, 329–343. [CrossRef]
17. Bull, A.M.J.; Katchburian, M.V.; Shih, Y.-F.; Amis, A.A. Standardisation of the description of patellofemoral motion and comparison between different techniques. *Knee Surg. Sports Traumatol. Arthrosc.* **2002**, *10*, 184–193. [CrossRef] [PubMed]
18. Grood, E.S.; Suntay, W.J. A joint coordinate system for the clinical description of three-dimensional motions: Application to the knee. *J. Biomech. Eng.* **1983**, *105*, 136–144. [CrossRef]

19. Innocenti, B.; Bori, E.; Piccolo, S. Development and validation of a robust patellar reference coordinate system for biomechanical and clinical studies. *Knee* **2020**, *27*, 81–88. [CrossRef]

20. Kebbach, M.; Darowski, M.; Krueger, S.; Schilling, C.; Grupp, T.M.; Bader, R.; Geier, A. Musculoskeletal Multibody Simulation Analysis on the Impact of Patellar Component Design and Positioning on Joint Dynamics after Unconstrained Total Knee Arthroplasty. *Materials* **2020**, *13*, 2365. [CrossRef]

21. Tischer, T.; Geier, A.; Lenz, R.; Woernle, C.; Bader, R. Impact of the patella height on the strain pattern of the medial patellofemoral ligament after reconstruction: A computer model-based study. *Knee Surg. Sports Traumatol. Arthrosc.* **2017**, *25*, 3123–3133. [CrossRef]

22. Woiczinski, M.; Steinbruck, A.; Weber, P.; Muller, P.E.; Jansson, V.; Schröder, C. Development and validation of a weight-bearing finite element model for total knee replacement. *Comput. Methods Biomech. Biomed. Engin.* **2016**, *19*, 1033–1045. [CrossRef]

23. Ahmed, A.M.; Duncan, N.A.; Tanzer, M. In Vitro Measurement of the Tracking Pattern of the Human Patella. *J. Biomech. Eng.* **1999**, *121*, 222–228. [CrossRef]

24. Hirokawa, S. Three-dimensional mathematical model analysis of the patellofemoral joint. *J. Biomech.* **1991**, *24*, 659–671. [CrossRef]

25. Hsu, H.-C.; Luo, Z.-P.; Rand, J.A.; An, K.-N. Influence of lateral release on patellar tracking and patellofemoral contact characteristics after total knee arthroplasty. *J. Arthroplasty* **1997**, *12*, 74–83. [CrossRef]

26. Koh, T.J.; Grabiner, M.D.; Swart, R.J.de. In vivo tracking of the human patella. *J. Biomech.* **1992**, *25*, 637–643. [CrossRef]

27. Lin, F.; Makhsous, M.; Chang, A.H.; Hendrix, R.W.; Zhang, L.-Q. In vivo and noninvasive six degrees of freedom patellar tracking during voluntary knee movement. *Clin. Biomech.* **2003**, *18*, 401–409. [CrossRef]

28. Anglin, C.; Ho, K.C.T.; Briard, J.-L.; de Lambilly, C.; Plaskos, C.; Nodwell, E.; Stindel, E. In vivo patellar kinematics during total knee arthroplasty. *Comput. Aided Surg.* **2008**, *13*, 377–391. [CrossRef]

29. Ali, A.A.; Mannen, E.M.; Rullkoetter, P.J.; Shelburne, K.B. In vivo comparison of medialized dome and anatomic patellofemoral geometries using subject-specific computational modeling. *J. Orthop. Res.* **2018**, *36*, 1910–1918. [CrossRef] [PubMed]

30. Wang, L.; Wang, C.J. Influence of patellar implantation on the patellofemoral joint of an anatomic customised total knee replacement implant: A case study. *Proc. Inst. Mech. Eng. H* **2020**, *234*, 1370–1383. [CrossRef] [PubMed]

31. Woernle, C. *Mehrkörpersysteme*; Springer: Berlin, Heidelberg, 2011; ISBN 978-3-642-15981-7.

32. Nigg, B.M. *Biomechanics of the Musculo-Skeletal System*, 2nd ed.; Wiley: Chichester, UK, 2002; ISBN 9780471978183.

33. Hemingway, E.G.; O'Reilly, O.M. Perspectives on Euler angle singularities, gimbal lock, and the orthogonality of applied forces and applied moments. *Multibody Syst. Dyn.* **2018**, *44*, 31–56. [CrossRef]

34. Cheung, R.T.H.; Mok, N.W.; Chung, P.Y.M.; Ng, G.Y.F. Non-invasive measurement of the patellofemoral movements during knee extension-flexion: A validation study. *Knee* **2013**, *20*, 213–217. [CrossRef] [PubMed]

35. Dagneaux, L.; Thoreux, P.; Eustache, B.; Canovas, F.; Skalli, W. Sequential 3D analysis of patellofemoral kinematics from biplanar x-rays: In vitro validation protocol. *Orthop. Traumatol. Surg. Res.* **2015**, *101*, 811–818. [CrossRef] [PubMed]

36. Merican, A.M.; Amis, A.A. Iliotibial band tension affects patellofemoral and tibiofemoral kinematics. *J. Biomech.* **2009**, *42*, 1539–1546. [CrossRef] [PubMed]

37. MacWilliams, B.A.; Davis, R.B. Addressing some misperceptions of the joint coordinate system. *J. Biomech. Eng.* **2013**, *135*, 54506. [CrossRef]

38. Lees, A.; Barton, G.; Robinson, M. The influence of Cardan rotation sequence on angular orientation data for the lower limb in the soccer kick. *J. Sports Sci.* **2010**, *28*, 445–450. [CrossRef]

39. Sinclair, J.; Hebron, J.; Hurst, H.; Taylor, P. The influence of different Cardan sequences on three-dimensional cycling kinematics. *Hum. Mov.* **2013**, *14*, 334–339. [CrossRef]

40. Ahmad, C.S.; Kwak, S.D.; Ateshian, G.A.; Warden, W.H.; Steadman, J.R.; Mow, V.C. Effects of patellar tendon adhesion to the anterior tibia on knee mechanics. *Am. J. Sports Med.* **1998**, *26*, 715–724. [CrossRef] [PubMed]

41. Suzuki, T.; Hosseini, A.; Li, J.-S.; Gill, T.J.; Li, G. In vivo patellar tracking and patellofemoral cartilage contacts during dynamic stair ascending. *J. Biomech.* **2012**, *45*, 2432–2437. [CrossRef]

42. Yeadon, M.R. The simulation of aerial movement—I. The determination of orientation angles from film data. *J. Biomech.* **1990**, *23*, 59–66. [CrossRef]

43. Sagan, B.E. *The Symmetric Group: Representations, Combinatorial Algorithms, and Symmetric Functions*, 2nd ed.; Springer: New York, NY, USA, 2010; ISBN 9781441928696.

44. Geier, A.; Aschemann, H.; Lima, D.D.; Woernle, C.; Bader, R. Force Closure Mechanism Modeling for Musculoskeletal Multibody Simulation. *IEEE Trans. Biomed. Eng.* **2018**, *65*, 2471–2482. [CrossRef]

45. Gale, T.; Anderst, W. Tibiofemoral helical axis of motion during the full gait cycle measured using biplane radiography. *Med. Eng. Phys.* **2020**, *86*, 65–70. [CrossRef]

46. Kwak, S.D.; Ahmad, C.S.; Gardner, T.R.; Grelsamer, R.P.; Henry, J.H.; Blankevoort, L.; Ateshian, G.A.; Mow, V.C. Hamstrings and iliotibial band forces affect knee kinematics and contact pattern. *J. Orthop. Res.* **2000**, *18*, 101–108. [CrossRef]

47. Yao, J.; Yang, B.; Niu, W.; Zhou, J.; Wang, Y.; Gong, H.; Ma, H.; Tan, R.; Fan, Y. In vivo measurements of patellar tracking and finite helical axis using a static magnetic resonance based methodology. *Med. Eng. Phys.* **2014**, *36*, 1611–1617. [CrossRef] [PubMed]

48. Rodrigues, O. Des lois géométriques qui régissent les déplacements d'unsystème solide dans l'espace, et de la variation des coordonnéesprovenant de ces déplacements considérés indépendammentdes causes qui peuvent les produire. *J. Math. Pures Appl.* **1840**, *5*, 380–440. (In French)

49. Bottema, O.; Roth, B. *Theoretical Kinematics*; Dover Publ: New York, NY, USA, 1990; ISBN 9780486663463.
50. Chirikjian, G.S.; Kyatkin, A.B. *Engineering Applications of Noncommutative Harmonic Analysis: With Emphasis on Rotation and Motion Groups*; CRC Press: Boca Raton, FL, USA, 2001; ISBN 9780849307485.
51. Woltring, H.J. 3-D attitude representation of human joints: A standardization proposal. *J. Biomech.* **1994**, *27*, 1399–1414. [CrossRef]
52. Fick, C.N.; Jiménez-Silva, R.; Sheehan, F.T.; Grant, C. Patellofemoral kinematics in patellofemoral pain syndrome: The influence of demographic factors. *J. Biomech.* **2021**, *130*, 110819. [CrossRef] [PubMed]
53. Ward, S.R.; Powers, C.M. The influence of patella alta on patellofemoral joint stress during normal and fast walking. *Clin. Biomech.* **2004**, *19*, 1040–1047. [CrossRef]
54. Pal, S.; Besier, T.F.; Beaupre, G.S.; Fredericson, M.; Delp, S.L.; Gold, G.E. Patellar maltracking is prevalent among patellofemoral pain subjects with patella alta: An upright, weightbearing MRI study. *J. Orthop. Res.* **2013**, *31*, 448–457. [CrossRef] [PubMed]
55. Shen, A.; Boden, B.P.; Grant, C.; Carlson, V.R.; Alter, K.E.; Sheehan, F.T. Adolescents and adults with patellofemoral pain exhibit distinct patellar maltracking patterns. *Clin. Biomech.* **2021**, *90*, 105481. [CrossRef] [PubMed]

6.   Publication III

scientific reports

Check for updates

OPEN

Isolated effects of patellar resurfacing in total knee arthroplasty and their relation to native patellar geometry

Adrian Sauer[1,2✉], Christoph Thorwaechter[2], Ingrid Dupraz[1], Allan Maas[1,2], Arnd Steinbrueck[2,3], Thomas M. Grupp[1,2] & Matthias Woiczinski[2]

The isolated effects of patellar resurfacing on patellar kinematics are rarely investigated. Nonetheless, knowing more about these effects could help to enhance present understanding of the emergence of kinematic improvements or deteriorations associated with patellar resurfacing. The aim of this study was to isolate the effects of patellar resurfacing from a multi-stage in vitro study, where kinematics after total knee arthroplasty before and after patellar resurfacing were recorded. Additionally, the influence of the native patellar geometry on these effects was analysed. Eight fresh frozen specimens were tested successively with different implant configurations on an already established weight bearing knee rig. The patello-femoral kinematics were thereby measured using an ultrasonic measurement system and its relation to the native patellar geometries was analysed. After patellar resurfacing, the specimen showed a significantly medialized patellar shift. This medialization of the patellar tracking was significantly correlated to the lateral facet angle of the native patella. The patellar shift after patellar resurfacing is highly influenced by the position of the patellar button and the native lateral patellar facet angle. As a result, the ideal medio-lateral position of the patellar component is affected by the geometry of the native patella.

In total knee arthroplasty (TKA), the question of whether or not to resurface the patella remains controversial[1,2]. There is evidence to indicate that patellar resurfacing can lead to both improved clinical outcomes and a reduced probability of revision surgery[1,3,4]. To identify and prove the effects of patellar resurfacing, functional analyses are shown to be more suitable than the established knee scores[5].

Detecting the isolated effects of patellar resurfacing on kinematics after TKA is a difficult task, mainly due to the high variation between subject kinematics. In order to address this limitation, a study aiming to characterize these effects must evaluate post-operative kinematics for a large enough cohort of patients, or, alternatively, assess knee kinematics after TKA both before and after patellar resurfacing. As a result, the studies that take on this objective are few and far between. Nevertheless, it is known that while patellar resurfacing has only minor effects on tibio-femoral kinematics[6,7] or gait patterns[8,9], it has been shown to influence patello-femoral kinematics[10] and tibio-femoral range of motion[11]. Additionally, it is possible to improve abnormal pre-operative patello-femoral motion patterns by navigated patellar resurfacing[12].

There are recommendations to medialize the patellar component on the patellar cut to restore the position of the patellar ridge[13], but since this medialization can cause an increase of lateral patellar tilt for some patients[14], the effect of the native patellar geometry on the optimal position of the patellar component needs to be further analysed.

The aim of this study was firstly to quantify the isolated effect of patellar resurfacing on patellar kinematics in an in vitro test setup for two different posterior stabilized implant variants. The hypotheses were that patellar kinematics are significantly influenced by patellar resurfacing but not by changing the tibiofemoral implant variants. Secondly the found effects were analysed and related to the native patellar geometries to enable a more nuanced view on the ideal placement of the patellar component in TKA.

[1]Aesculap AG, Research and Development, Am Aesculap-Platz, 78532 Tuttlingen, Germany. [2]Ludwig Maximilians University Munich, Department of Orthopaedic and Trauma Surgery, Musculoskeletal University Center Munich (MUM), University Hospital, Munich, Germany. [3]Orthopaedic Surgical Competence Center Augsburg (OCKA), Augsburg, Germany. ✉email: Adrian.Sauer@aesculap.de

Materials and methods

Specimens and implantation. For this study, eight fresh frozen specimens, (5 male, 3 female, age 52 ± 16 years, 7 left and 1 right) with less than 10° of varus or valgus and without severe bone deformities, were used. The implantation and testing process was the same as described in earlier studies[15–20]. The tibia and femur were cut 22 cm and 20 cm from the epicondylar line, respectively, and were embedded into pots with epoxy resin (RenCast FC 52/53 Isocyanate & FC 53 Polyol, Huntsman Advanced Materials GmbH, Texas, USA) The fibula head was fixed in the proximal tibia with a cortical screw. The vastus medialis, vastus lateralis, semitendinosus, rectus femoris and biceps femoris were attached to metallic finger traps (Bühler-Instrumente Medizintechnik GmbH, Tuttlingen, Germany) to apply muscle forces in the knee rig.

The posterior stabilized implants (Vega PS System, Aesculap AG, Tuttlingen, Germany) were placed in tibia-first technique with an intramedullary alignment. The femoral medio-lateral position was centred to the femoral bone, while its rotation was aligned to the anatomical trans-epicondylar axis. The used femoral implant has the same radius in the cavity of the trochlea as the dome-shaped patellar button. Therefore, full congruency is reached in the artificial patello-femoral joint. To increase the resistance against lateral subluxation of the patella, the lateral flange is slightly more pronounced than the medial one.

To implant the patellar button in a second surgery step after kinematic testing of the native patella, the thickness of the patellar button was resected and the medio-lateral position of the patellar implant was centred on the surface of the bone cut. No medialization of the patellar button was performed.

With every specimen several trials were executed. Before implantation the native knee was tested. After the implantation of the tibiofemoral implants, trials with a PS and a PS+ inlay were executed with the native and resurfaced patella, respectively.

Knee rig. A well-established weight bearing knee rig[15–20] which performs a squat from 30° to 130° moving 3°/s, was used for testing. To measure the flexion angle, two angular sensors (8820, Burster, Gernsbach, Germany) placed at the hip and ankle joint were used. For each of the three bone segments of the knee joint, the movements of four bony landmarks were recorded with an ultrasonic measurement system (Zebris CMS20, Isny, Germany). These landmarks allow the mapping of the anatomic reference frames to the femur, tibia and patella bones.

The resolution of the sensors is 0.1° and 0.1 mm. The reliability was measured previously with seven specimen, three cycles each, where the mean standard deviation was 0.2 mm for patellar shift, 0.5° for patellar flexion and 0.2° for patellar spin and tilt, respectively.

The rig is shown in Fig. 1 and applies passive forces of 20 N to the vastus medialis, vastus lateralis, semitendinosus and the biceps femoris, while the force of the rectus femoris is actively controlled to reach 50 N of ground reaction force at the ankle joint (FN 7325–31, FGP Sensors & Instrumentation, Les Clayes Sous Bois, France). LabView was used for real time test control (Version 8.6, National Instruments, Austin, TX, USA).

Data analysis. From the recorded trajectories of the landmarks, the patello-femoral kinematics were calculated for every trial using Matlab (MathWorks Inc., Natick, MA, USA). Patello-femoral kinematics are described using the three-cylinder-open-chain method[21,22], where a positive patellar shift is given if the patella translates along the femoral flexion axis to the lateral side. Patellar flexion, tilt and spin are the rotations of the patella around the femoral flexion axis, the patellar long-axis and the floating axis between these two, respectively.

Since effects caused by the differences between the specimens would cover effects of the different implant configurations, only differences to the native situation, termed relative kinematics, are analysed within this study.

For every specimen, an MRI-scan (Siemens Aera, Siemens AG, Munich, Germany) was executed. The native MRI was executed with frozen specimens to avoid an additional defrosting cycle. Therefore, it was not possible to control the knee flexion angle in an accurate manner for the MRI scans. All scans were executed between full extension and 30° of flexion. Four parallel planes, which were orthogonal to the sagittal plane and equidistantly distributed between the proximal and distal end of the patella, were defined within these scans. For these planes, the angle between the tangent of the lateral facet and the patellar plane was measured, as shown in Fig. 2. The average of all measurements for every specimen was used as the lateral patellar facet angle α_l.

A linear regression model was calculated to analyse the relationship between the lateral patellar facet angle and the difference in patellar shift. An F-Test was executed to test if the slope of this regression function differs significantly from zero.

Ethics statement. This study was approved by the ethics committee of the University of Munich, Germany (approval 58–16) and carried out in accordance with relevant guidelines and regulations. Informed consent for donation to scientific research had been signed before death by the donors or after death by their relatives.

Results

For the patellar kinematics relative to the native knee, no significant differences between the Vega PS and PS+ inserts were found. The comparison between the implant configurations with resurfaced and native patella also showed no significant differences for patellar rotations (patellar flexion, tilt and spin). The average curve of the patellar shift for all specimens with resurfaced patella is outside of the 95%-confidence intervals (CI) for native patella and vice versa, as shown in Fig. 3. Therefore, the patellar shift after patellar resurfacing is significantly lower than before, indicating a more medial patellar tracking after resurfacing. The averaged medialization for the full load cycle after patellar resurfacing is 2.7 ± 1.2 mm. For these isolated effects of patellar resurfacing, no significant difference was found between male and female specimens.
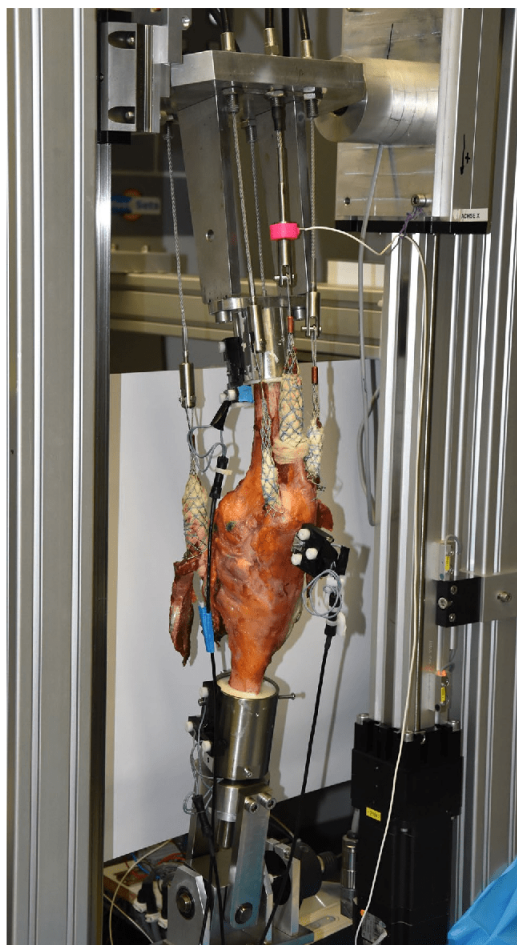
Figure 1. One of the specimens mounted on the knee rig.

In a linear regression model, the lateral facet angle explains 72.9% (PS+) and 39.4% (PS) of the variance of the averaged difference in the patellar shift before and after patellar resurfacing. If Vega PS and PS+ are combined in one dataset, 53.7% of the variance in the averaged patellar shift difference were explained by a (highly) significant ($p = 0.001$) linear regression function of the lateral facet angle. A higher lateral facet angle is related to a more lateral patella tracking after resurfacing and to a decreased difference in patellar shift before and after patellar resurfacing. The data and linear regression function are shown in Fig. 4.

Discussion

The objective of this study was to analyse patello-femoral kinematics and how they are influenced by differing implant configurations, with a special focus given to the effects of patellar resurfacing. The posterior-stabilized Vega implants were tested with PS and PS+ inlays before and after patellar resurfacing, respectively. The difference in the PS and PS+ tibial inlays did not change patello-femoral kinematics in a significant way, either in the native stage nor in the patellar resurfaced stage. Placing the patellar button significantly affected patellar tracking, which was medialized with the resurfaced patella. Patello-femoral rotations were not significantly affected by patellar resurfacing.

Patellar resurfacing led to a significant difference in patellar shift. For a given femoral implant, a resurfaced patella will, on average, be medialized by 2.7 ± 1.2 mm when compared to the native patella. Ostermeier et al. came to similar results in their in vitro study, where the maximum medialization of the patella increased by 3 mm after resurfacing even though the patella was placed with 5 mm of medialization[10].

The present study has demonstrated that the described difference in patellar shift can be associated with the lateral patellar facet angle, such that 53.7% of patellar shift variance can be explained by this specific parameter.
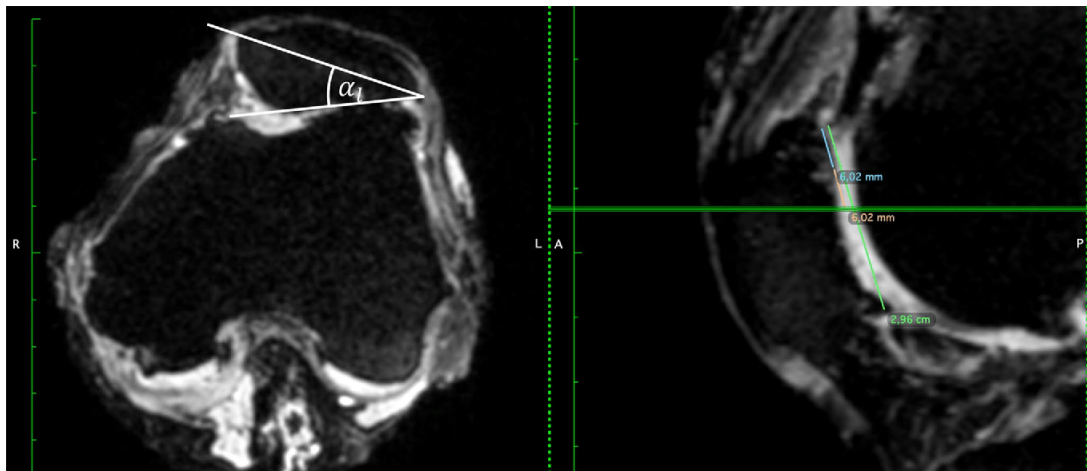
Figure 2. Visualization of the angles measured in the MRI data of the native knee joint. Left: patello-femoral joint in view from distal with measured lateral patellar facet angle. Right: sagittal view with the actual plane for the distal view (green). The angle drawn in the left image was measured in four parallel and equidistant planes of the patella.
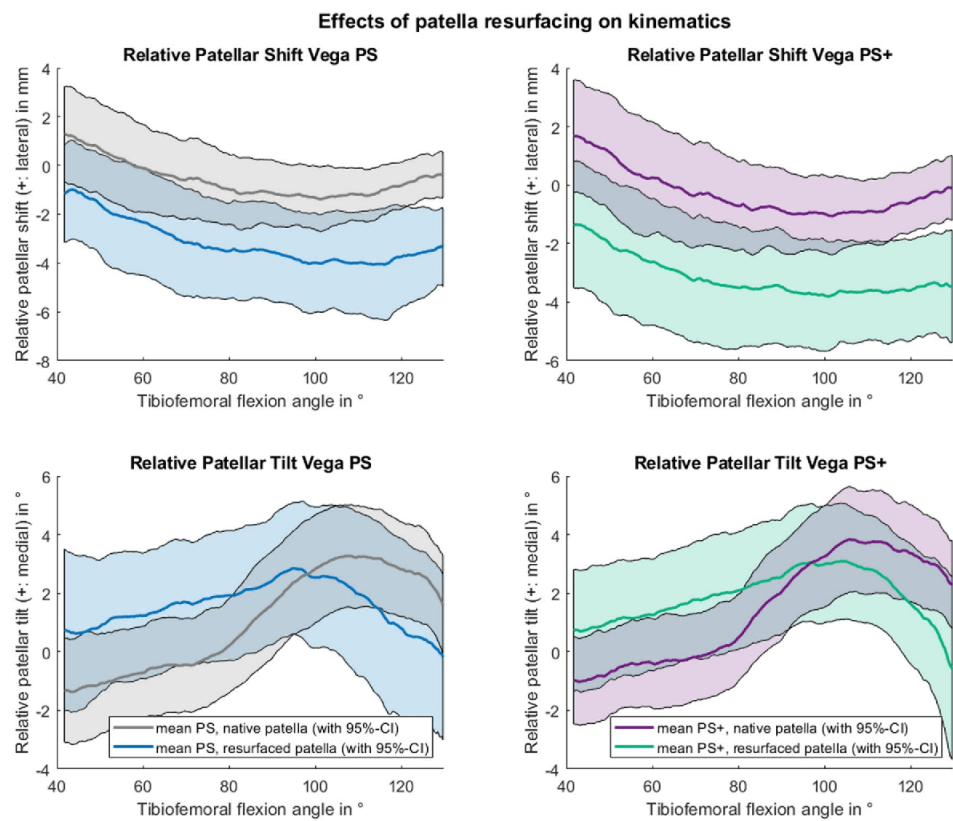

Figure 3. Differences to the native situation for patellar shift (top) and tilt (lower) with Vega PS (left) and PS+ (right) inserts for native (grey/purple) and resurfaced patella (blue/green).
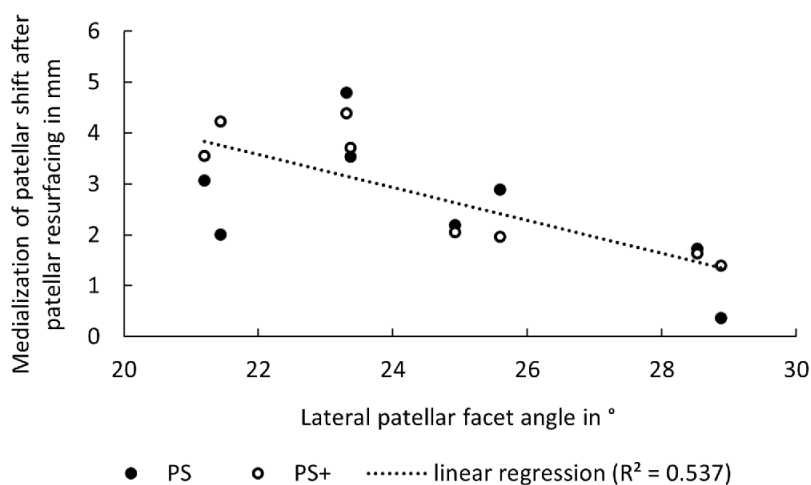
Figure 4. Dot plot showing the connection between the average difference of patellar shift before and after patellar resurfacing and the lateral patellar facet angle for PS and PS+. The linear regression model for all these values shows, that 53.7% of the variance in the patellar shift difference can be explained by the lateral facet angle.

This relationship can be caused by the underlying surgical protocol, where the patellar button position was centred on the bone cut surface. Using this method, a small lateral facet angle leads to an overstuffing of the patellar button on the native lateral facet, as is illustrated in Fig. 5. Therefore, the patella is forced to be medialized.

The present study has some limitations. Firstly, the deep knee bend was performed with a constant ground reaction force of 50 N and secondly, it must be mentioned that this is an in-vitro study with a small sample size. Furthermore, measuring the native lateral patellar facet angle can be very inaccurate for cases with advanced arthritis. This would prevent surgeons from applying the results of this study.

From our study, we can conclude that resurfacing the patella without medialization could lead to a change in patellar shift. For specimens with pronounced patellar facet asymmetry, where the medial facet is more steep than the lateral one, this effect seems to be particularly evident. To reduce changes in patellar shift, the patellar button can be placed with a tendency towards the side, where the native facet with the higher angle was located. Since the medial facet angle usually tends to be higher than the lateral one, a slight offset of the patellar button to the medial side, as has been often recommended[23,24], shall prove to be a favourable choice in the majority of cases. It was reported earlier that medialization of the patellar component can reduce the patellofemoral contact force and lateral retinacular tension, as well as the frequency of its release[25]. This could be explained by the described lateral overstuffing of the patellar component and the resulting medialization of the patella tracking found in this study.

A surgeon's first inclination to avoid lateral subluxation of the patella might be to favour a lateral placement of the patellar button, which would lead to overall medialization of the patella tracking. However, the results of this study show that, in fact, this medialization of the entire patella can just as successfully be achieved by opting for a central button positioning. This effect was especially notable in cases where the lateral patellar facet angle was small.

Conclusions
Based on our results, it could be worth to consider the native patellar geometry to choose the medio-lateral position of the patellar implant, and thus minimize the deviation from patellar kinematics without patellar resurfacing. Further research needs to be done to analyse how to determine the medio-lateral implant position in everyday clinical workflows.
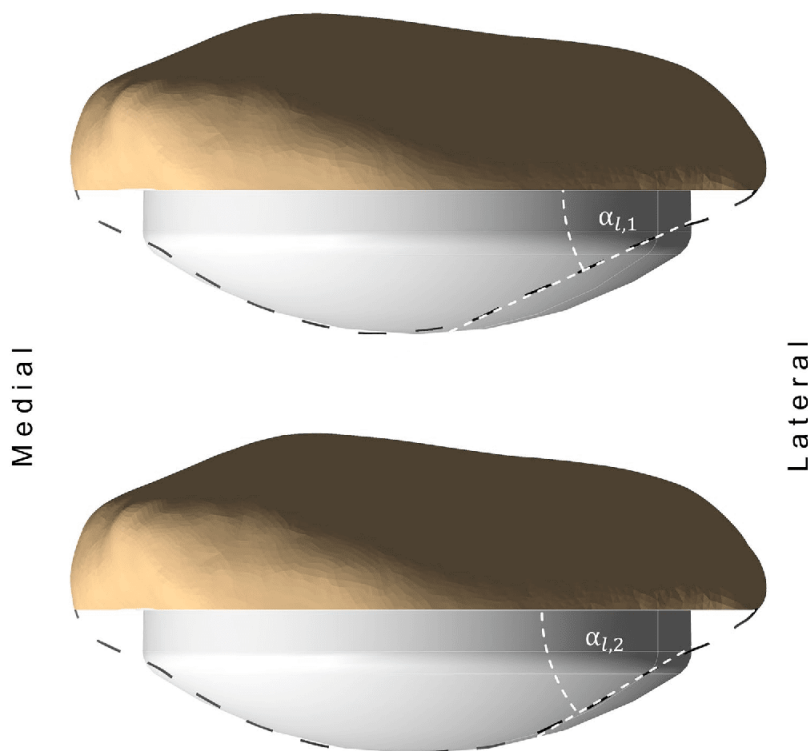
Figure 5. Lateral overstuffing for patellae with different native lateral facet angles with a centrally placed dome-shaped patellar component. For a small lateral facet angle $\alpha_{l,1}$, the lateral overstuffing increases (top) compared to a bigger native lateral facet angle $\alpha_{l,2}$ (lower).

Data availability
The datasets generated and analysed during the current study are available from the corresponding author on reasonable request.

References
1. Grassi, A. *et al.* Patellar resurfacing versus patellar retention in primary total knee arthroplasty: A systematic review of overlapping meta-analyses. *Knee Surg. Sports Traumatol. Arthrosc.* **26**, 3206–3218 (2018).
2. McConaghy, K. *et al.* Patellar management during total knee arthroplasty: A review. *EFORT Open Rev.* **6**, 861–871 (2021).
3. van der Merwe, J. M. & Mastel, M. S. Controversial topics in total knee arthroplasty: a 5-year update (part 1). *J. Am. Acad. Orthop. Surg. Glob. Res. Rev.* **4**, e1900047 (2020).
4. Li, S. *et al.* Systematic review of patellar resurfacing in total knee arthroplasty. *Int. Orthop.* **35**, 305–316 (2011).
5. van Hemert, W. L. W. *et al.* Patella retention versus replacement in total knee arthroplasty; functional and clinimetric aspects. *Arch. Orthop. Trauma Surg.* **129**, 259–265 (2009).
6. Kono, K. *et al.* Patellar resurfacing has minimal impact on in vitro tibiofemoral kinematics during deep knee flexion in total knee arthroplasty. *Knee* **30**, 163–169 (2021).
7. Belvedere, C. *et al.* Does navigated patellar resurfacing in total knee arthroplasty result in proper bone cut, motion and clinical outcomes?. *Clin. Biomech. (Bristol, Avon)* **69**, 168–177 (2019).
8. Smith, A. J., Lloyd, D. G. & Wood, D. J. A kinematic and kinetic analysis of walking after total knee arthroplasty with and without patellar resurfacing. *Clin. Biomech. (Bristol, Avon)* **21**, 379–386 (2006).
9. Xu, Y., Bai, Y., Zhou, J., Li, Q. & Liang, J. Gait analysis in primary total knee arthroplasty with and without patellar resurfacing: A randomized control study. *J. Shanghai Jiaotong Univ. (Sci.)* **15**, 632–636 (2010).
10. Ostermeier, S., Buhrmester, O., Hurschler, C. & Stukenborg-Colsman, C. Dynamic in vitro measurement of patellar movement after total knee arthroplasty: An in vitro study. *BMC Musculoskelet. Disord.* **6**, 30 (2005).
11. Berti, L., Benedetti, M. G., Ensini, A., Catani, F. & Giannini, S. Clinical and biomechanical assessment of patella resurfacing in total knee arthroplasty. *Clin. Biomech. (Bristol, Avon)* **21**, 610–616 (2006).
12. Belvedere, C. *et al.* Tibio-femoral and patello-femoral joint kinematics during navigated total knee arthroplasty with patellar resurfacing. *Knee Surg. Sports Traumatol. Arthrosc.* **22**, 1719–1727 (2014).

13. Hofmann, A. A., Tkach, T. K., Evanich, C. J., Camargo, M. P. & Zhang, Y. Patellar component medialization in total knee arthroplasty. *J. Arthroplasty* **12**, 155–160 (1997).
14. Nikolaus, O. B., Larson, D. R., Hanssen, A. D., Trousdale, R. T. & Sierra, R. J. Lateral patellar facet impingement after primary total knee arthroplasty: It does exist. *J. Arthroplasty* **29**, 970–976 (2014).
15. Bauer, L. *et al*. Secondary patellar resurfacing in TKA: A combined analysis of registry data and biomechanical testing. *J. Clin. Med.* **10**, 1227 (2021).
16. Dupraz, I. *et al*. Impact of femoro-tibial size combinations and TKA design on kinematics. *Arch. Orthop. Trauma Surg.* https://doi.org/10.1007/s00402-021-03923-y (2021).
17. Steinbruck, A. *et al*. Influence of tibial rotation in total knee arthroplasty on knee kinematics and retropatellar pressure: An in vitro study. *Knee Surg. Sports Traumatol. Arthrosc.* **24**, 2395–2401 (2016).
18. Steinbrück, A. *et al*. Femorotibial kinematics and load patterns after total knee arthroplasty. An in vitro comparison of posterior-stabilized versus medial-stabilized design. *Clin. Biomech. (Bristol, Avon)* **33**, 42–48 (2016).
19. Steinbrück, A. *et al*. A lateral retinacular release during total knee arthroplasty changes femorotibial kinematics: An in vitro study. *Arch. Orthop. Trauma Surg.* **138**, 401–407 (2018).
20. Steinbruck, A. *et al*. Influence of mediolateral tibial baseplate position in TKA on knee kinematics and retropatellar pressure. *Knee Surg. Sports Traumatol. Arthrosc.* https://doi.org/10.1007/s00167-015-3843-x (2015).
21. Bull, A. M. J., Katchburian, M. V., Shih, Y.-F. & Amis, A. A. Standardisation of the description of patellofemoral motion and comparison between different techniques. *Knee Surg. Sports Traumatol. Arthrosc.* **10**, 184–193 (2002).
22. Sauer, A., Kebbach, M., Maas, A., Mihalko, W. M. & Grupp, T. M. The influence of mathematical definitions on patellar kinematics representations. *Materials (Basel, Switzerland)* **14**, 7644 (2021).
23. Anglin, C. *et al*. Biomechanical consequences of patellar component medialization in total knee arthroplasty. *J. Arthroplasty* **25**, 793–802 (2010).
24. Kawano, T. *et al*. Factors affecting patellar tracking after total knee arthroplasty. *J. Arthroplasty* **17**, 942–947 (2002).
25. Lee, R. H., Jeong, H. W., Lee, J. K. & Choi, C. H. Should the position of the patellar component replicate the vertical median ridge of the native patella?. *Knee* **24**, 82–90 (2017).

Author contributions

Funding

Competing interests

Additional information

Correspondence and requests for materials should be addressed to A.Sa.

Reprints and permissions information is available at www.nature.com/reprints.

Publisher's note Springer Nature remains neutral with regard to jurisdictional claims in published maps and institutional affiliations.

7. References

1. Meftah, M., Ranawat, A. S. & Ranawat, C. S. Safety and efficacy of a rotating-platform, high-flexion knee design three- to five-year follow-up. *The Journal of Arthroplasty* **27,** 201–206 (2012).

2. Baker, P. N., van der Meulen, J. H., Lewsey, J. & Gregg, P. J. The role of pain and function in determining patient satisfaction after total knee replacement. Data from the National Joint Registry for England and Wales. *The Journal of Bone and Joint Surgery. British volume* **89,** 893–900 (2007).

3. Breugem, S. J. M. & Haverkamp, D. Anterior knee pain after a total knee arthroplasty: What can cause this pain? *World Journal of Orthopedics* **5,** 163–170 (2014).

4. Putman, S., Boureau, F., Girard, J., Migaud, H. & Pasquier, G. Patellar complications after total knee arthroplasty. *Orthopaedics & Traumatology, Surgery & Research : OTSR* **105,** S43-S51 (2019).

5. Johnson, D. P. & Eastwood, D. M. Patellar complications after knee arthroplasty. A prospective study of 56 cases using the Kinematic prosthesis. *Acta Orthopaedica Scandinavica* **63,** 74–79 (1992).

6. Freeman, M. A., Todd, R. C., Bamert, P. & Day, W. H. ICLH arthroplasty of the knee: 1968--1977. *The Journal of Bone and Joint Surgery. British volume* **60-B,** 339–344 (1978).

7. Park, C. N., White, P. B., Meftah, M., Ranawat, A. S. & Ranawat, C. S. Diagnostic Algorithm for Residual Pain After Total Knee Arthroplasty. *Orthopedics* **39,** e246-52 (2016).

8. Bergmann, G., Bender, A., Graichen, F., Dymke, J., Rohlmann, A., Trepczynski, A., Heller, M. O. & Kutzner, I. Standardized loads acting in knee implants. *PloS one* **9,** e86035 (2014).

9. D'Lima, D. D., Townsend, C. P., Arms, S. W., Morris, B. A. & Colwell, C. W. An implantable telemetry device to measure intra-articular tibial forces. *Journal of Biomechanics* **38,** 299–304 (2005).

10. Heinlein, B., Graichen, F., Bender, A., Rohlmann, A. & Bergmann, G. Design, calibration and pre-clinical testing of an instrumented tibial tray. *Journal of Biomechanics* **40 Suppl 1,** S4-10 (2007).

11. Churchill, D. L., Incavo, S. J., Johnson, C. C. & Beynnon, B. D. The influence of femoral roll-back on patellofemoral contact loads in total knee arthroplasty. *The Journal of Arthroplasty* **16,** 909–918 (2001).

12. Cohen, Z. A., Roglic, H., Grelsamer, R. P., Henry, J. H., Levine, W. N., Mow, V. C. & Ateshian, G. A. Patellofemoral stresses during open and closed kinetic chain exercises. An analysis using computer simulation. *The American Journal of Sports Medicine* **29,** 480–487 (2001).

13. Petersilge, W. J., Oishi, C. S., Kaufman, K. R., Irby, S. E. & Colwell, C. W. The effect of trochlear design on patellofemoral shear and compressive forces in total knee arthroplasty. *Clinical Orthopaedics and Related Research,* 124–130 (1994).

14. Townsend, P. R., Rose, R. M., Radin, E. L. & Raux, P. The biomechanics of the human patella and its implications for chondromalacia. *Journal of Biomechanics* **10,** 403–407 (1977).

15. Singerman, R., Davy, D. T. & Goldberg, V. M. Effects of patella alta and patella infera on patellofemoral contact forces. *Journal of Biomechanics* **27,** 1059–1065 (1994).

16. Singerman, R., Berilla, J., Archdeacon, M. & Peyser, A. In vitro forces in the normal and cruciate-deficient knee during simulated squatting motion. *Journal of Biomechanical Engineering* **121,** 234–242 (1999).

17. Lewallen, D. G., Riegger, C. L., Myers, E. R. & Hayes, W. C. Effects of retinacular release and tibial tubercle elevation in patellofemoral degenerative joint disease. *J. Orthop. Res.* **8,** 856–862 (1990).

18. Upadhyay, N., Vollans, S. R., Seedhom, B. B. & Soames, R. W. Effect of patellar tendon shortening on tracking of the patella. *The American Journal of Sports Medicine* **33,** 1565–1574 (2005).

19. Mason, J. J., Leszko, F., Johnson, T. & Komistek, R. D. Patellofemoral joint forces. *Journal of Biomechanics* **41,** 2337–2348 (2008).

20. Müller, O., Lo, J., Wünschel, M., Obloh, C. & Wülker, N. Simulation of force loaded knee movement in a newly developed in vitro knee simulator. *Biomedizinische Technik. Biomedical engineering* **54,** 142–149 (2009).

21. Dahlkvist, N. J., Mayo, P. & Seedhom, B. B. Forces during squatting and rising from a deep squat. *Engineering in Medicine* **11,** 69–76 (1982).

22. Reilly, D. T. & Martens, M. Experimental Analysis of the Quadriceps Muscle Force and Patello-Femoral Joint Reaction Force for Various Activities. *Acta Orthopaedica Scandinavica* **43,** 126–137 (1972).

23. Heino Brechter, J. & Powers, C. M. Patellofemoral stress during walking in persons with and without patellofemoral pain. *Medicine & Science in Sports & Exercise* **34,** 1582–1593 (2002).

24. Ward, S. R. & Powers, C. M. The influence of patella alta on patellofemoral joint stress during normal and fast walking. *Clinical Biomechanics (Bristol, Avon)* **19,** 1040–1047 (2004).

25. Kebbach, M., Darowski, M., Krueger, S., Schilling, C., Grupp, T. M., Bader, R. & Geier, A. Musculoskeletal Multibody Simulation Analysis on the Impact of Patellar Component Design and Positioning on Joint Dynamics after Unconstrained Total Knee Arthroplasty. *Materials (Basel, Switzerland)* **13** (2020).

26. Trepczynski, A., Kutzner, I., Kornaropoulos, E., Taylor, W. R., Duda, G. N., Bergmann, G. & Heller, M. O. Patellofemoral joint contact forces during activities with high knee flexion. *Journal of Orthopaedic Research* **30,** 408–415 (2012).

27. Latypova, A., Arami, A., Becce, F., Jolles-Haeberli, B., Aminian, K., Pioletti, D. P. & Terrier, A. A patient-specific model of total knee arthroplasty to estimate patellar strain: A case study. *Clinical Biomechanics* **32,** 212–219 (2016).

28. Harlaar, J., Eenkhoorn, C. & Macri, E. Patellofemoral joint contact forces at different activities - effects of modeling assumptions. *Osteoarthritis and Cartilage* **28,** 252 (2020).

29. Shelburne, K. B., Torry, M. R. & Pandy, M. G. Muscle, Ligament, and Joint-Contact Forces at the Knee during Walking. *Medicine & Science in Sports & Exercise* **37,** 1948–1956 (2005).

30. Hart, H. F., Patterson, B. E., Crossley, K. M., Culvenor, A. G., Khan, M. C. M., King, M. G. & Sritharan, P. May the force be with you: understanding how patellofemoral joint reaction force

compares across different activities and physical interventions-a systematic review and meta-analysis. *British journal of sports medicine* **56,** 521–530 (2022).

31. Burroughs, B. R., Rubash, H. E., Estok, D., Jasty, M., Krevolin, J. & Muratoglu, O. K. Comparison of conventional and highly crosslinked UHMWPE patellae evaluated by a new in vitro patellofemoral joint simulator. *Journal of biomedical materials research. Part B, Applied biomaterials* **79,** 268–274 (2006).

32. Ellison, P., Barton, D. C., Esler, C., Shaw, D. L., Stone, M. H. & Fisher, J. In vitro simulation and quantification of wear within the patellofemoral joint replacement. *Journal of Biomechanics* **41,** 1407–1416 (2008).

33. Maiti, R., Cowie, R. M., Fisher, J. & Jennings, L. M. The influence of malalignment and ageing following sterilisation by gamma irradiation in an inert atmosphere on the wear of ultra-high-molecular-weight polyethylene in patellofemoral replacements. *Proceedings of the Institution of Mechanical Engineers. Part H, Journal of engineering in medicine* **231,** 634–642 (2017).

34. Maiti, R., Fisher, J., Rowley, L. & Jennings, L. M. The influence of kinematic conditions and design on the wear of patella-femoral replacements. *Proceedings of the Institution of Mechanical Engineers. Part H, Journal of engineering in medicine* **228,** 175–181 (2014).

35. Vambiervliet, J., Bellemans, J., Verlinden, C., Luyckx, J.-P., Labey, L., Innocenti, B. & Vandenneucker, H. The influence of malrotation and femoral component material on patellofemoral wear during gait. *The Journal of Bone and Joint Surgery. British volume,* 1348–1354 (2011).

36. Lewis, G. Properties of crosslinked ultra-high-molecular-weight polyethylene. *Biomaterials* **22,** 371–401 (2001).

37. Oral, E. & Muratoglu, O. K. Radiation cross-linking in ultra-high molecular weight polyethylene for orthopaedic applications. *Nuclear instruments & methods in physics research. Section B, Beam interactions with materials and atoms* **265,** 18–22 (2007).

38. Australian Orthopaedic Association National Joint Replacement Registry. *Hip, Knee & Shoulder Arthroplasty. Annual Report 2022* (Australian Orthopaedic Association, 2022). Figure KT5, Tables KT44 and KT51.

39. Australian Orthopaedic Association National Joint Replacement Registry. *Hip, Knee & Shoulder Arthroplasty. Annual Report 2020* (Australian Orthopaedic Association, 2020). Table KT44.

40. German Society for Orthopaedics and Orthopaedic Surgery. *The German Arthroplasty Registry (EPRD). Annual Report 2021* (EPRD Deutsche Endoprothesenregister gGmbH, 2021). Table 38.

41. *The National Joint Registry 18th Annual Report 2021* (National Joint Registry, 2021). Table 3.K7.

42. Seth, A., Hicks, J. L., Uchida, T. K., Habib, A., Dembia, C. L., Dunne, J. J., Ong, C. F., DeMers, M. S., Rajagopal, A., Millard, M., Hamner, S. R., Arnold, E. M., Yong, J. R., Lakshmikanth, S. K., Sherman, M. A., Ku, J. P. & Delp, S. L. OpenSim: Simulating musculoskeletal dynamics and neuromuscular control to study human and animal movement. *PLoS computational biology* **14,** e1006223 (2018).

43. Herrmann, S., Kluess, D., Kaehler, M., Grawe, R., Rachholz, R., Souffrant, R., Zierath, J., Bader, R. & Woernle, C. A Novel Approach for Dynamic Testing of Total Hip Dislocation under Physiological Conditions. *PloS one* **10,** e0145798 (2015).

44. Michaud, F., Lamas, M., Lugrís, U. & Cuadrado, J. A fair and EMG-validated comparison of recruitment criteria, musculotendon models and muscle coordination strategies, for the inverse-dynamics based optimization of muscle forces during gait. *Journal of neuroengineering and rehabilitation* **18,** 17 (2021).

45. Prilutsky, B. I. & Zatsiorsky, V. M. Optimization-based models of muscle coordination. *Exercise and sport sciences reviews* **30,** 32–38 (2002).

46. Sauer, A., Maas, A., Ottawa, S., Giurea, A. & Grupp, T. M. Towards a New, Pre-Clinical, Subject-Independent Test Model for Kinematic Analysis after Total Knee Arthroplasty—Influence of the Proximo-Distal Patella Position and Patellar Tendon Stiffness. *Applied Sciences* **11,** 1–16 (2021).

47. van Kampen, A. & Huiskes, R. The three-dimensional tracking pattern of the human patella. *Journal of orthopaedic research : official publication of the Orthopaedic Research Society* **8,** 372–382 (1990).

48. Omori, G., Koga, Y., Bechtold, J. E., Gustilo, R. B., Nakabe, N., Sasagawa, K., Hara, T. & Takahashi, H. E. Contact pressure and three-dimensional tracking of unresurfaced patella in total knee arthroplasty. *The Knee* **4,** 15–21 (1997).

49. Sakai, N., Luo, Z.-P., Rand, J. A. & An, K.-N. Quadriceps forces and patellar motion in the anatomical model of the patellofemoral joint. *The Knee* **3,** 1–7 (1996).

50. Sakai, N., Luo, Z.-P., Rand, J. A. & An, K.-N. The influence of weakness in the vastus medialis oblique muscle on the patellofemoral joint: an in vitro biomechanical study. *Clinical Biomechanics* **15,** 335–339 (2000).

51. Chew, J. T., Stewart, N. J., Hanssen, A. D., Luo, Z.-P., Rand, J. A. & An, K.-N. Differences in Patellar Tracking and Knee Kinematics Among Three Different Total Knee Designs. *Clinical Orthopaedics and Related Research* **345,** 87-98 (1997).

52. Cheung, R. T. H., Mok, N. W., Chung, P. Y. M. & Ng, G. Y. F. Non-invasive measurement of the patellofemoral movements during knee extension-flexion: a validation study. *The Knee* **20,** 213–217 (2013).

53. Suzuki, T., Hosseini, A., Li, J.-S., Gill, T. J. & Li, G. In vivo patellar tracking and patellofemoral cartilage contacts during dynamic stair ascending. *Journal of Biomechanics* **45,** 2432–2437 (2012).

54. Dagneaux, L., Thoreux, P., Eustache, B., Canovas, F. & Skalli, W. Sequential 3D analysis of patellofemoral kinematics from biplanar x-rays: In vitro validation protocol. *Orthopaedics & Traumatology, Surgery & Research : OTSR* **101,** 811–818 (2015).

55. Bull, A. M. J., Katchburian, M. V., Shih, Y.-F. & Amis, A. A. Standardisation of the description of patellofemoral motion and comparison between different techniques. *Knee surgery, sports traumatology, arthroscopy : official journal of the ESSKA* **10,** 184–193 (2002).

56. Grood, E. S. & Suntay, W. J. A joint coordinate system for the clinical description of three-dimensional motions: application to the knee. *Journal of Biomechanical Engineering* **105,** 136–144 (1983).

57. Sauer, A., Kebbach, M., Maas, A., Mihalko, W. M. & Grupp, T. M. The Influence of Mathematical Definitions on Patellar Kinematics Representations. *Materials (Basel, Switzerland)* **14,** 1–15 (2021).

58. Katchburian, M. V., Bull, A. M. J., Shih, Y.-F., Heatley, F. W. & Amis, A. A. Measurement of patellar tracking: assessment and analysis of the literature. *Clinical Orthopaedics and Related Research,* 241–259 (2003).

59. Yu, Z., Yao, J., Wang, X., Xin, X., Zhang, K., Cai, H., Fan, Y. & Yang, B. Research Methods and Progress of Patellofemoral Joint Kinematics: A Review. *Journal of healthcare engineering* **2019,** 9159267 (2019).

60. Taylor, W. R., Schütz, P., Bergmann, G., List, R., Postolka, B., Hitz, M., Dymke, J., Damm, P., Duda, G., Gerber, H., Schwachmeyer, V., Hosseini Nasab, S. H., Trepczynski, A. & Kutzner, I. A comprehensive assessment of the musculoskeletal system. The CAMS-Knee data set. *Journal of Biomechanics* **65,** 32–39 (2017).

61. Vandenneucker, H., Labey, L., Vander Sloten, J., Desloovere, K. & Bellemans, J. Isolated patellofemoral arthroplasty reproduces natural patellofemoral joint kinematics when the patella is resurfaced. *Knee surgery, sports traumatology, arthroscopy : official journal of the ESSKA* **24,** 3668–3677 (2016).

62. Ahmed, A. M., Duncan, N. A. & Tanzer, M. In Vitro Measurement of the Tracking Pattern of the Human Patella. *Journal of Biomechanical Engineering* **121,** 222–228 (1999).

63. Hofmann, A. A., Tkach, T. K., Evanich, C. J., Camargo, M. P. & Zhang, Y. Patellar component medialization in total knee arthroplasty. *The Journal of Arthroplasty* **12,** 155–160 (1997).

64. Kawano, T., Miura, H., Nagamine, R., Urabe, K., Matsuda, S., Mawatari, T., Moro-Oka, T. & Iwamoto, Y. Factors affecting patellar tracking after total knee arthroplasty. *The Journal of Arthroplasty* **17,** 942–947 (2002).

65. Myles, C. M., Rowe, P. J., Nutton, R. W. & Burnett, R. The effect of patella resurfacing in total knee arthroplasty on functional range of movement measured by flexible electrogoniometry. *Clinical Biomechanics (Bristol, Avon)* **21,** 733–739 (2006).

66. Smith, A. J., Lloyd, D. G. & Wood, D. J. A kinematic and kinetic analysis of walking after total knee arthroplasty with and without patellar resurfacing. *Clinical Biomechanics (Bristol, Avon)* **21,** 379–386 (2006).

67. Xu, Y., Bai, Y., Zhou, J., Li, Q. & Liang, J. Gait analysis in primary total knee arthroplasty with and without patellar resurfacing: A randomized control study. *J. Shanghai Jiaotong Univ. (Sci.)* **15,** 632–636 (2010).

68. Anglin, C., Brimacombe, J. M., Wilson, D. R., Masri, B. A., Greidanus, N. V., Tonetti, J. & Hodgson, A. J. Biomechanical consequences of patellar component medialization in total knee arthroplasty. *The Journal of Arthroplasty* **25,** 793–802 (2010).

69. Belvedere, C., Ensini, A., Leardini, A., Dedda, V., Feliciangeli, A., Cenni, F., Timoncini, A., Barbadoro, P. & Giannini, S. Tibio-femoral and patello-femoral joint kinematics during navigated total knee arthroplasty with patellar resurfacing. *Knee Surgery, Sports Traumatology, Arthroscopy* **22,** 1719–1727 (2014).

70. Ostermeier, S., Buhrmester, O., Hurschler, C. & Stukenborg-Colsman, C. Dynamic in vitro measurement of patellar movement after total knee arthroplasty: an in vitro study. *BMC musculoskeletal disorders* **6,** 30 (2005).

71. Steinbrück, A., Schröder, C., Woiczinski, M., Fottner, A., Müller, P. E. & Jansson, V. Patellofemoral contact patterns before and after total knee arthroplasty: an in vitro measurement. *Biomedical Engineering Online* **12,** 58 (2013).

72. Steinbruck, A., Schröder, C., Woiczinski, M., Fottner, A., Muller, P. E. & Jansson, V. The effect of trochlea tilting on patellofemoral contact patterns after total knee arthroplasty: an in vitro study. *Archives of orthopaedic and trauma surgery* **134,** 867–872 (2014).

73. Steinbrück, A., Woiczinski, M., Weber, P., Müller, P. E., Jansson, V. & Schröder, C. Posterior cruciate ligament balancing in total knee arthroplasty: a numerical study with a dynamic force controlled knee model. *Biomedical Engineering Online* **13,** 91 (2014).

74. Steinbruck, A., Schröder, C., Woiczinski, M., Muller, T., Muller, P. E., Jansson, V. & Fottner, A. Influence of tibial rotation in total knee arthroplasty on knee kinematics and retropatellar pressure: an in vitro study. *Knee Surgery, Sports Traumatology, Arthroscopy* **24,** 2395–2401 (2016).

75. Steinbrück, A., Schröder, C., Woiczinski, M., Glogaza, A., Müller, P. E., Jansson, V. & Fottner, A. A lateral retinacular release during total knee arthroplasty changes femorotibial kinematics: an in vitro study. *Archives of orthopaedic and trauma surgery* **138,** 401–407 (2018).

76. Dupraz, I., Thorwächter, C., Grupp, T. M., Hammerschmid, F., Woiczinski, M., Jansson, V., Müller, P. E. & Steinbrück, A. Impact of femoro-tibial size combinations and TKA design on kinematics. *Archives of orthopaedic and trauma surgery*; 10.1007/s00402-021-03923-y (2021).

77. Bauer, L., Woiczinski, M., Thorwächter, C., Melsheimer, O., Weber, P., Grupp, T. M., Jansson, V. & Steinbrück, A. Secondary Patellar Resurfacing in TKA: A Combined Analysis of Registry Data and Biomechanical Testing. *Journal of clinical medicine* **10** (2021).

78. Woiczinski, M., Steinbruck, A., Weber, P., Muller, P. E., Jansson, V. & Schröder, C. Development and validation of a weight-bearing finite element model for total knee replacement. *Computer Methods in Biomechanics and Biomedical Engineering* **19,** 1033–1045 (2016).

79. Sauer, A., Thorwaechter, C., Dupraz, I., Maas, A., Steinbrueck, A., Grupp, T. M. & Woiczinski, M. Isolated effects of patellar resurfacing in total knee arthroplasty and their relation to native patellar geometry. *Scientific reports* **12** (2022).